Psychedelics Promote Structural and Functional Neural Plasticity

by

Calvin Ly[1], Alexandra C. Greb[1], Lindsay P. Cameron[2], Jonathan M. Wong[2], Eden V. Barragan[2], Paige C. Wilson[3], Kyle F. Burbach[4], Sina Soltanzadeh Zarandi[1], Alexander Sood[5], Michael R. Paddy[3], Whitney C. Duim[1], Megan Y. Dennis[4,6,7], A. Kimberley McAllister[5,8,9], Kassandra M. Ori-McKenney[3], John A. Gray[5,8], and David E. Olson[1,5,6,10,*]

Ly *et al.*, 2018, Cell Reports 23, 3170-3182

June 12, 2018
https://doi.org/10.1016/j.celrep.2018.05.022

original report: https://www.cell.com/cell-reports/pdfExtended/S2211-1247(18)30755-1

[1]Department of Chemistry, University of California, Davis, Davis, CA 95616, USA
[2]Neuroscience Graduate Program, University of California, Davis, Davis, CA 95618, USA
[3]Department of Molecular and Cellular Biology, University of California, Davis, Davis, CA 95616, USA
[4]Genome Center, University of California, Davis, Davis, CA 95616, USA
[5]Center for Neuroscience, University of California, Davis, Davis, CA 95618, USA
[6]Department of Biochemistry and Molecular Medicine, School of Medicine, University of California, Davis, Sacramento, CA 95817, USA
[7]MIND Institute, University of California, Davis, Sacramento, CA 95817, USA
[8]Department of Neurology, School of Medicine, University of California, Davis, Sacramento, CA 95817, USA
[9]Department of Neurobiology, Physiology, and Behavior, University of California, Davis, Davis, CA 95616, USA
[10]Lead Contact
[*]Correspondence: deolson@ucdavis.edu

Table of Contents:

Summary
Introduction
Results
Psychedelics Promote Neuritogenesis
Psychedelics Promote Spinogenesis and Synaptogenesis
Psychedelics Promote Plasticity through a TrkBand mTOR-Dependent Mechanism
The 5-HT2A Receptor Mediates the Effects of Psychedelics on Structural Plasticity
Discussion
Experimental Procedures
Drugs
Animals
Cell Culture
Statistical Analysis
Acknowledgments
Author Contributions
Declaration of Interests
References
Supplemental Information
Supplemental Methods
Drugs
Neuritogenesis Experiments
Spinogenesis Experiments

Synaptogenesis Experiments
ELISA
ddPCR
5-HT2A Staining Experiments
Drosophila Experiments
Zebrafish Experiments
Golgi-Cox Staining
Electrophysiology
Code Availability
Data Availability
Supplemental References

Graphical Abstract

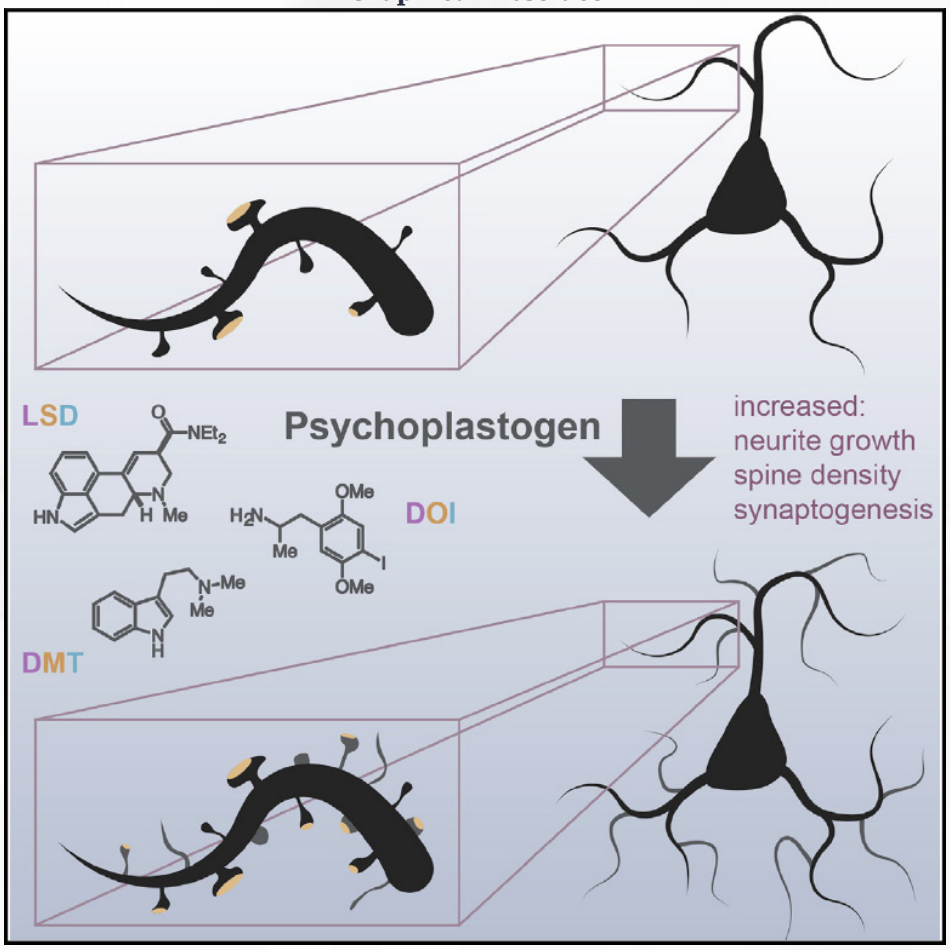

Summary

Atrophy of neurons in the prefrontal cortex (PFC) plays a key role in the pathophysiology of depression and related disorders. The ability to promote both structural and functional plasticity in the PFC has been hypothesized to underlie the fast-acting antidepressant properties of the dissociative anesthetic ketamine. Here, we report that, like ketamine, serotonergic psychedelics are capable of robustly increasing neuritogenesis and/or spinogenesis both *in vitro* and *in vivo*. These changes in neuronal structure are accompanied by increased synapse number and function, as measured by fluorescence microscopy and electrophysiology. The structural changes induced by psychedelics appear to result from stimulation of the TrkB, mTOR, and 5-HT_{2A} signaling pathways and could possibly explain the clinical effectiveness of these compounds. Our results underscore the therapeutic potential of psychedelics and, importantly, identify several lead scaffolds for medicinal chemistry efforts focused on developing plasticity-promoting compounds as safe, effective, and fast-acting treatments for depression and related disorders.

Introduction

Neuropsychiatric diseases, including mood and anxiety disorders, are some of the leading causes of disability worldwide and place an enormous economic burden on society (Gustavsson *et al*., 2011; Whiteford *et al*., 2013). Approximately one-third of patients will not respond to current antidepressant drugs, and those who do will usually require at least 2-4 weeks of treatment before they experience any beneficial effects (Rush *et al*., 2006). Depression, post-traumatic stress disorder (PTSD), and addiction share common neural circuitry (Arnsten, 2009; Russo *et al*., 2009; Peters *et al*., 2010; Russo and Nestler, 2013) and have high comorbidity (Kelly and Daley, 2013). A preponderance of evidence from a combination of human imaging, postmortem studies, and animal models suggests that atrophy of neurons in the prefrontal cortex (PFC) plays a key role in the pathophysiology of depression and related disorders and is precipitated and/or exacerbated by stress (Arnsten, 2009; Autry and Monteggia, 2012; Christoffel *et al*., 2011; Duman and Aghajanian, 2012; Duman *et al*., 2016; Izquierdo *et al*., 2006; Pittenger and Duman, 2008; Qiao *et al*., 2016; Russo and Nestler, 2013). These structural changes, such as the retraction of neurites, loss of dendritic spines, and elimination of synapses, can potentially be counteracted by compounds capable of promoting structural and functional neural plasticity in the PFC (Castrén and Antila, 2017; Cramer *et al*., 2011; Duman, 2002; Hayley and Litteljohn, 2013; Kolb and Muhammad, 2014; Krystal *et al*., 2009; Mathew *et al*., 2008), providing a general solution to treating all of these related diseases. However, only a relatively small number of compounds capable of promoting plasticity in the PFC have been identified so far, each with significant drawbacks (Castrén and Antila, 2017). Of these, the dissociative anesthetic ketamine has shown the most promise, revitalizing the field of molecular psychiatry in recent years.

Ketamine has demonstrated remarkable clinical potential as a fast-acting antidepressant (Berman *et al*., 2000; Ionescu *et al*., 2016; Zarate *et al*., 2012), even exhibiting efficacy in treatment-resistant populations (Diaz-Granados *et al*., 2010; Murrough *et al*., 2013; Zarate *et al*., 2006). Additionally, it has shown promise for treating PTSD (Feder *et al*., 2014) and heroin addiction (Krupitsky *et al*., 2002). Animal models suggest that its therapeutic effects stem from its ability to promote the growth of dendritic spines, increase the synthesis of synaptic proteins, and strengthen synaptic responses (Autry *et al*., 2011; Browne and Lucki, 2013; Li *et al*., 2010).

Like ketamine, serotonergic psychedelics and entactogens have demonstrated rapid and long-lasting antidepressant and anxiolytic effects in the clinic after a single dose (Bouso *et al*., 2008; Carhart-Harris and Goodwin, 2017; Grob *et al*., 2011; Mithoefer *et al*., 2013, 2016; Nichols *et al*., 2017; Sanches *et al*., 2016; Osório *et al*., 2015), including in treatment-resistant populations (Carhart-Harris *et al*., 2016, 2017; Mithoefer *et al*., 2011; Oehen *et al*., 2013; Rucker *et al*., 2016). In fact, there have been numerous clinical trials in the past 30 years examining the therapeutic effects of these drugs (Dos Santos *et al*., 2016), with 3,4-methylenedioxymethamphetamine (MDMA) recently receiving the "breakthrough therapy" designation by the Food and Drug Administration for treating PTSD. Furthermore, classical psychedelics and entactogens produce antidepressant and anxiolytic responses in rodent behavioral tests, such as the forced swim test (Cameron *et al*., 2018) and fear extinction learning (Cameron *et al*., 2018; Catlow *et al*., 2013; Young *et al*., 2015), paradigms for which ketamine has also been shown to be effective (Autry *et al*., 2011; Girgenti *et al*., 2017; Li *et al*., 2010). Despite the promising antidepressant, anxiolytic, and anti-addictive properties of serotonergic psychedelics, their therapeutic mechanism of action remains poorly understood, and concerns about safety have severely limited their clinical usefulness.

Because of the similarities between classical serotonergic psychedelics and ketamine in both preclinical models and clinical studies, we reasoned that their therapeutic effects might result from a shared ability to promote structural and functional neural plasticity in cortical neurons. Here, we report that serotonergic psychedelics and entactogens from a variety of chemical classes (e.g., amphetamine, tryptamine, and ergoline) display plasticity-promoting properties comparable to or greater than ketamine. Like ketamine, these compounds stimulate structural plasticity by activating the mammalian target of rapamycin (mTOR). To classify the growing number of compounds capable of rapidly promoting induced plasticity (Castrén and Antila, 2017), we introduce the term "psychoplastogen," from the Greek roots psych- (mind), -plast (molded), and -gen (producing). Our work strengthens the growing body of literature indicating that psychoplastogens capable of promoting plasticity in the PFC might have value as fast-acting antidepressants and anxiolytics with efficacy in treatment-resistant populations and suggests that it may be possible to use classical psychedelics as

lead structures for identifying safer alternatives.

Results

Psychedelics Promote Neuritogenesis

Because atrophy of cortical neurons is believed to be a contributing factor to the development of mood and anxiety disorders (Christoffel *et al.*, 2011; Duman and Aghajanian, 2012), we first treated cultured cortical neurons with psychedelics from a variety of structural classes (Figures 1A and S1A) and measured the resulting changes in various morphological features. Using Sholl analysis (Ristanović *et al.*, 2006), we observed that several psychedelics increased dendritic arbor complexity comparably to ketamine, as measured by the area under the curve of the Sholl plots as well as the maximum number of crossings (Figures 1B-1E and S1B-S1E). This increase in arbor complexity appeared to result from large changes in both the number of dendritic branches and the total length of the arbors (Figures 1F, 1H, S1F, and S1H). Psychedelics had a limited effect on the number of primary dendrites and did not alter the length of the longest dendrite (Figures 1G, 1I, S1G, and S1I).

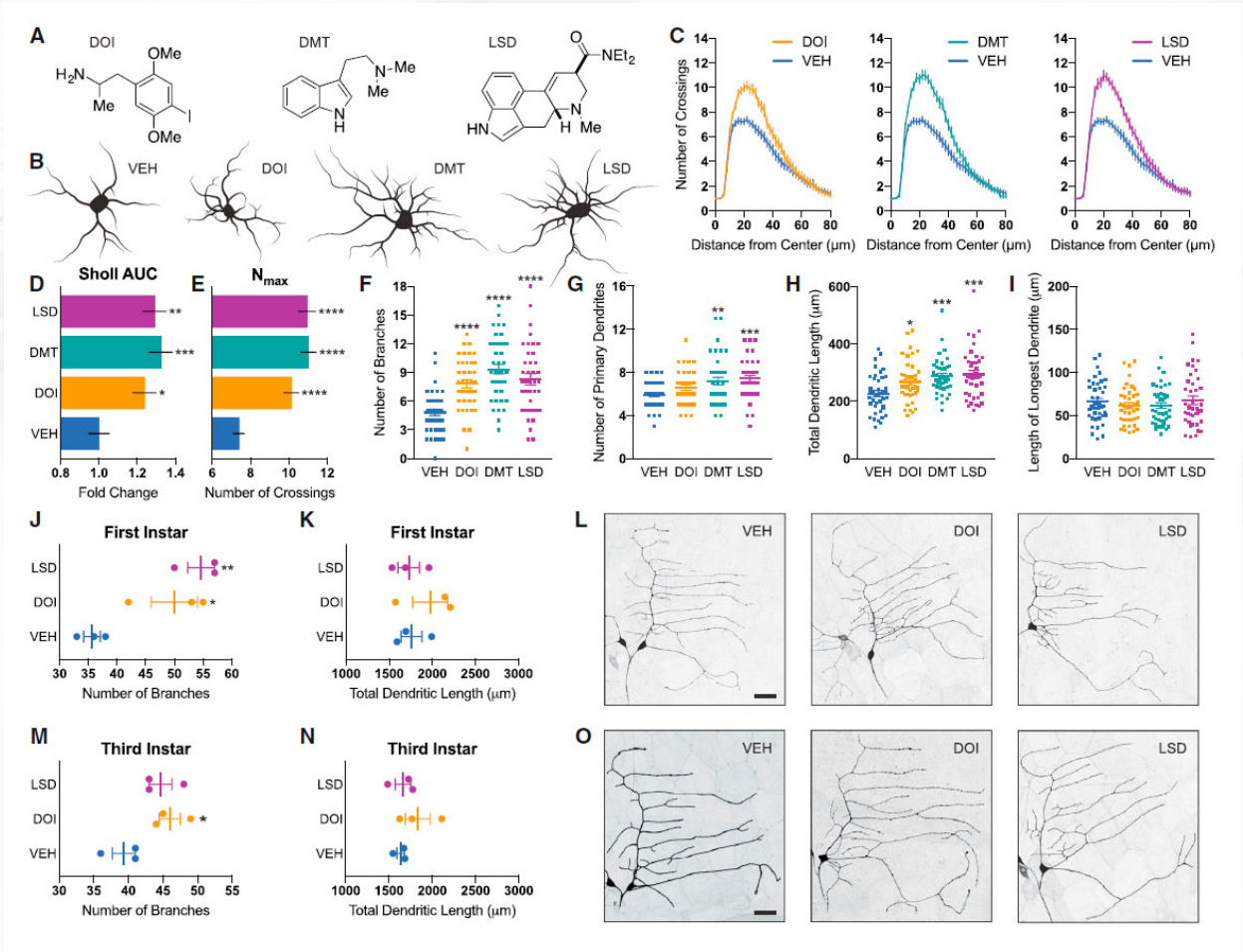

Figure 1. Psychedelics Promote Neuritogenesis both *In Vitro* and *In Vivo*
(A) Chemical structures of psychedelics.
(B) Representative tracings of cortical neurons (DIV6) treated with compounds.
(C) Sholl analysis demonstrates that psychedelics increase dendritic arbor complexity (n = 39-41 neurons).
(D) Area under the curve (AUC) of the Sholl plots in (C).
(E) Maximum number of crossings (N_{max}) of the Sholl plots in (C).
(F-I) Cortical neurons treated with psychedelics display an increase in the number of branches (F), the number of primary dendrites (G), and the total length of the dendritic arbor (H) but not the length of the longest dendrite (I).
(J and K) Class I neurons from *Drosophila* larvae treated with psychedelics during the first instar display increased branching (J) but not total length of the dendritic arbor (K) (n = 3 neurons).
(L) Representative images of neurons from (J) and (K).
(M and N) Class I neurons from *Drosophila* larvae treated with psychedelics during the third instar display increased branching (M) but not total length of the dendritic arbor (N) (n = 3 neurons).
(O) Representative images from (M) and (N).
*p < 0.05, **p < 0.01, ***p < 0.001, ****p < 0.0001, as compared to vehicle control (VEH). Scale bars, 30 μm. Data are represented as mean ± SEM. See also Figures S1-S5.

Nearly all psychedelic compounds tested were capable of robustly promoting neuritogenesis, with comparable effects being produced by tryptamines (*N*,*N*-dimethyltryptamine [DMT] and psilocin), amphetamines (2,5-dimethoxy-4-iodoamphetamine [DOI] and MDMA), and ergolines (lysergic acid diethylamide [LSD]). As a positive control, we treated cells with 7,8-dihydroxyflavone (DHF), a psychoplastogen structurally dissimilar to classical psychedelics (Jang *et al*., 2010), and found that it also increased dendritic arbor complexity (Figure S2). This neurite outgrowth structural phenotype seems to only be induced by select compounds because serotonin and D-amphetamine, molecules that are chemically related to classical psychedelics and entactogens, exerted minimal to no effects on neuritogenesis (Figure S2).

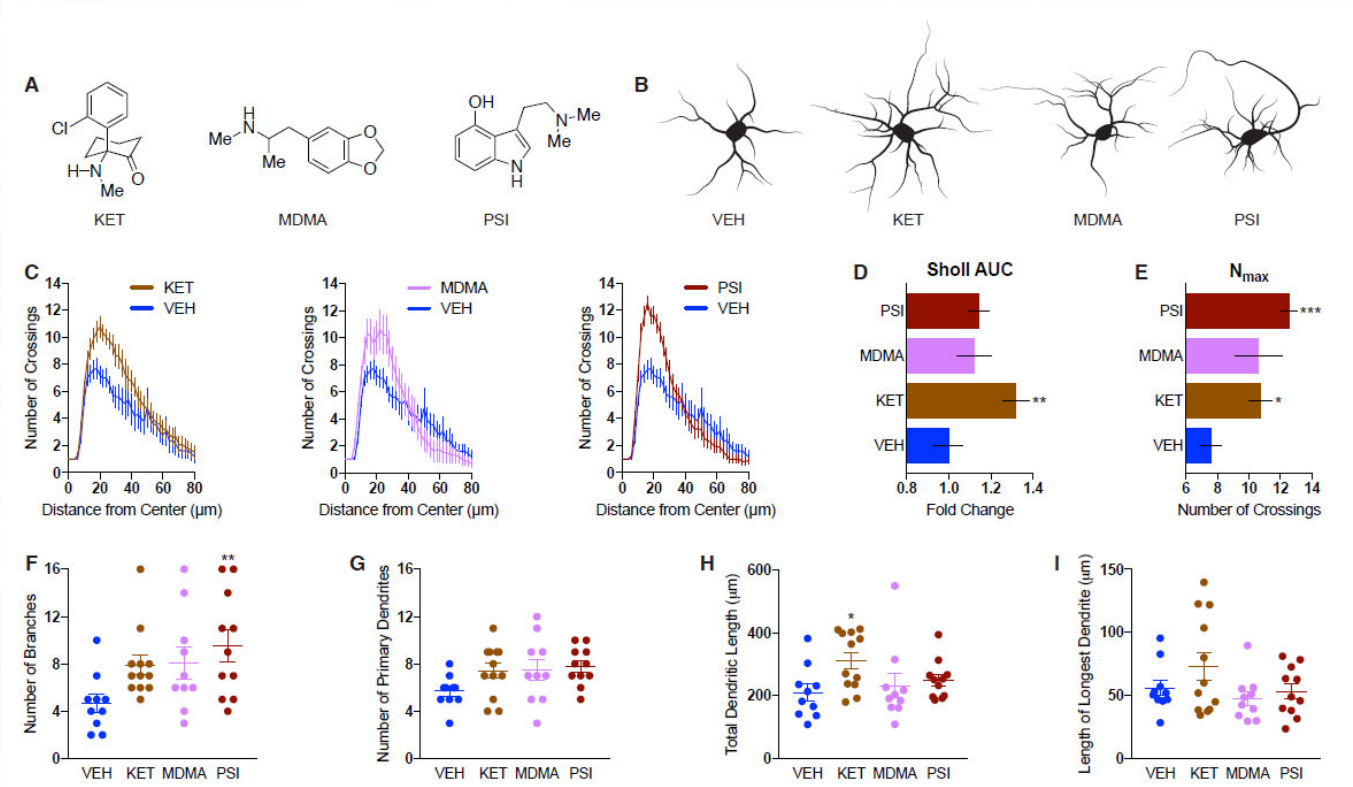

Figure S1. Psychedelics Promote Neuritogenesis (Additional Compounds), Related to Figure 1. (A) Chemical structures of additional psychedelics used in these studies. (B) Representative tracings of cultured embryonic rat cortical neurons (DIV6) treated with compounds. (C) Sholl analysis (circle radii = 2 μm increments) demonstrates that cultured cortical neurons treated with several psychedelics have more complex dendritic arbors as compared to vehicle control (n = 10-12 neurons per treatment). (D) Area under the curve (AUC) of the Sholl plots in C. (E) Maximum number of crossings (N_{max}) of the Sholl plots in C. (F-I) Cultured cortical neurons treated with several psychedelics display a trend towards an increase in the number of branch points (F), the number of primary dendrites (G), and the total length of the dendritic arbor (H), but not the length of the longest dendrite (I). Error bars represent s.e.m. *p < 0.05, **p < 0.01, ***p < 0.001, as compared to vehicle control (One-way ANOVA with Dunnett's post-hoc test). VEH = vehicle, KET= ketamine, MDMA = (±)-3,4-methylenedioxymethamphetamine, PSI = psilocin.

To establish the relative potencies and efficacies of hallucinogens and entactogens for promoting neurite outgrowth, we conducted 8-point dose-response studies (Figure S3). We defined 100% and 0% efficacy as the maximum number of crossings induced by ketamine (10 μM) and vehicle (0.1% DMSO), respectively. We chose the 10 μM concentration of ketamine as the upper limit because this concentration of ketamine is reached in the brain following intraperitoneal administration of an antidepressant dose in rats (Yang *et al*., 2018). For consistency, we used this same concentration when testing the effects of psychedelics and entactogens, with DMT being the only exception. We used a maximum 90 μM concentration of DMT in our studies to more closely mimic the brain concentration of DMT in rats treated with an antidepressant dose (Cohen and Vogel, 1972; Cameron *et al*., 2018). In this neuritogenesis assay, ketamine's half maximal effective concentration (EC_{50}) value was 132 nM. Surprisingly, the majority of the psychedelics and entactogens we tested exhibited significantly greater potency than ketamine, with LSD being particularly potent (EC_{50} = 0.409 nM). In fact, LSD exhibited activity across 8 orders of magnitude into the low picomolar range (Figure S3).

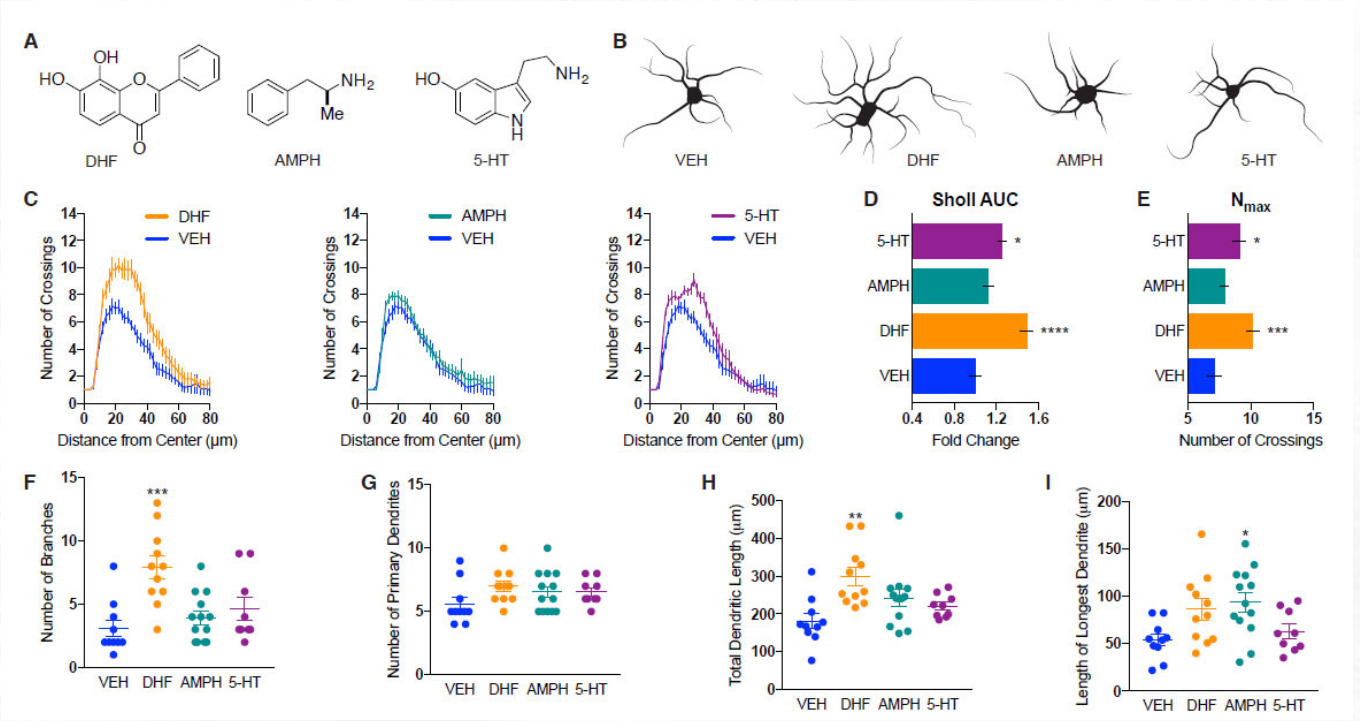

Figure S2. Structural Plasticity is Promoted by a TrkB Agonist, but Not a Psychostimulant or Monoamine Neurotransmitter Structurally Related to Classical Psychedelics, Related to Figure 1. (A) Chemical structures of control compounds used in these studies (DHF = positive control, AMPH and 5HT = negative controls). (B) Representative tracings of cultured embryonic rat cortical neurons (DIV6) treated with compounds. (C) Sholl analysis (circle radii = 2 μm increments) demonstrates that cultured cortical neurons treated with DHF, a TrkB agonist, have more complex dendritic arbors as compared to vehicle control. However, AMPH and 5-HT were not able to elicit a similar response (n = 9-13 neurons per treatment). (D) Area under the curve (AUC) of the Sholl plots in C. (E) Maximum number of crossings (N_{max}) of the Sholl plots in C. (F-I) Cultured cortical neurons treated with DHF, but not AMPH or 5-HT, exhibited an increased number of branch points (F) and total length of the dendritic arbor (H), but minimal changes in the number of primary dendrites (G) or the length of the longest dendrite (I). Error bars represent s.e.m. *$p < 0.05$, **$p < 0.01$, ***$p < 0.001$, ****$p < 0.0001$ as compared to vehicle control (One-way ANOVA with Dunnett's post-hoc test). VEH = vehicle, AMPH = D-Amphetamine, 5-HT = 5-hydroxytryptamine (serotonin), DHF = 7,8-dihydroxyflavone.

Notably, the anti-addictive alkaloid ibogaine (Alper, 2001; Belgers *et al*., 2016) was the only psychedelic tested that had absolutely no effect (Figure S4). This was a surprising result because we hypothesized that ibogaine's long-lasting antiaddictive properties might result from its psychoplastogenic properties. Previous work by He *et al*. (2005) clearly demonstrated that ibogaine increases the expression of glial cell linederived neurotrophic factor (GDNF) and that this plasticity-promoting protein is critical to ibogaine's anti-addictive mechanism of action. Because several reports have suggested that noribogaine, a metabolite of ibogaine, might actually be the active compound *in vivo* (Zubaran *et al*., 1999; Baumann *et al*., 2000, 2001), we decided to test its ability to promote neuritogenesis in cultured cortical neurons. Gratifyingly, noribogaine robustly increased dendritic arbor complexity with an EC_{50} value comparable to ketamine (Figure S3), providing additional evidence suggesting that it may be the active compound *in vivo*.

To assess the *in vivo* effects of classical psychedelics on neuritogenesis, we started treating *Drosophila* larvae during the first instar with LSD and DOI. As observed in rodent cortical cultures, both LSD and DOI significantly increased dendritic branching of class I sensory neurons; however, they did not increase the total length of the dendritic arbors (Figures 1J-1L). Because of the striking effects of psychedelics on the structures of immature neurons, we hypothesized that they might influence neurodevelopment. To test this, we chronically treated zebrafish embryos with compounds for 6 days immediately following dechorionation and assessed gross morphological changes and behavior. We did not observe any differences in head sizes between the treatment groups, nor did we detect any statistically significant differences in activity levels (Figure S5). Next we assessed the ability of psychedelics to promote neuritogenesis in more mature neurons by starting to treat *Drosophila* larvae during the late second instar. Again, psychedelics increased the branching of class I neurons, although the effect was less dramatic than that observed when treatment was started during the first instar (Figure 1M-1O). Although different developmental stages might be more or less susceptible to the effects of psychedelics, it is also possible that the smaller effect size observed after administering compounds starting at the later time point was simply the result of treating the larvae for a shorter period of time. Regardless, it was quite surprising to observe compound-induced changes in neuronal structure after initiating treatment during the late second instar because class I neurons are stereotyped and typically possess relatively few higher-order branches (Grueber *et al*., 2002). Moreover, our results demonstrate that

psychedelics can promote changes in neuronal structure across vertebrate (rats) and invertebrate (*Drosophila*) species, suggesting that they act through an evolutionarily conserved mechanism.

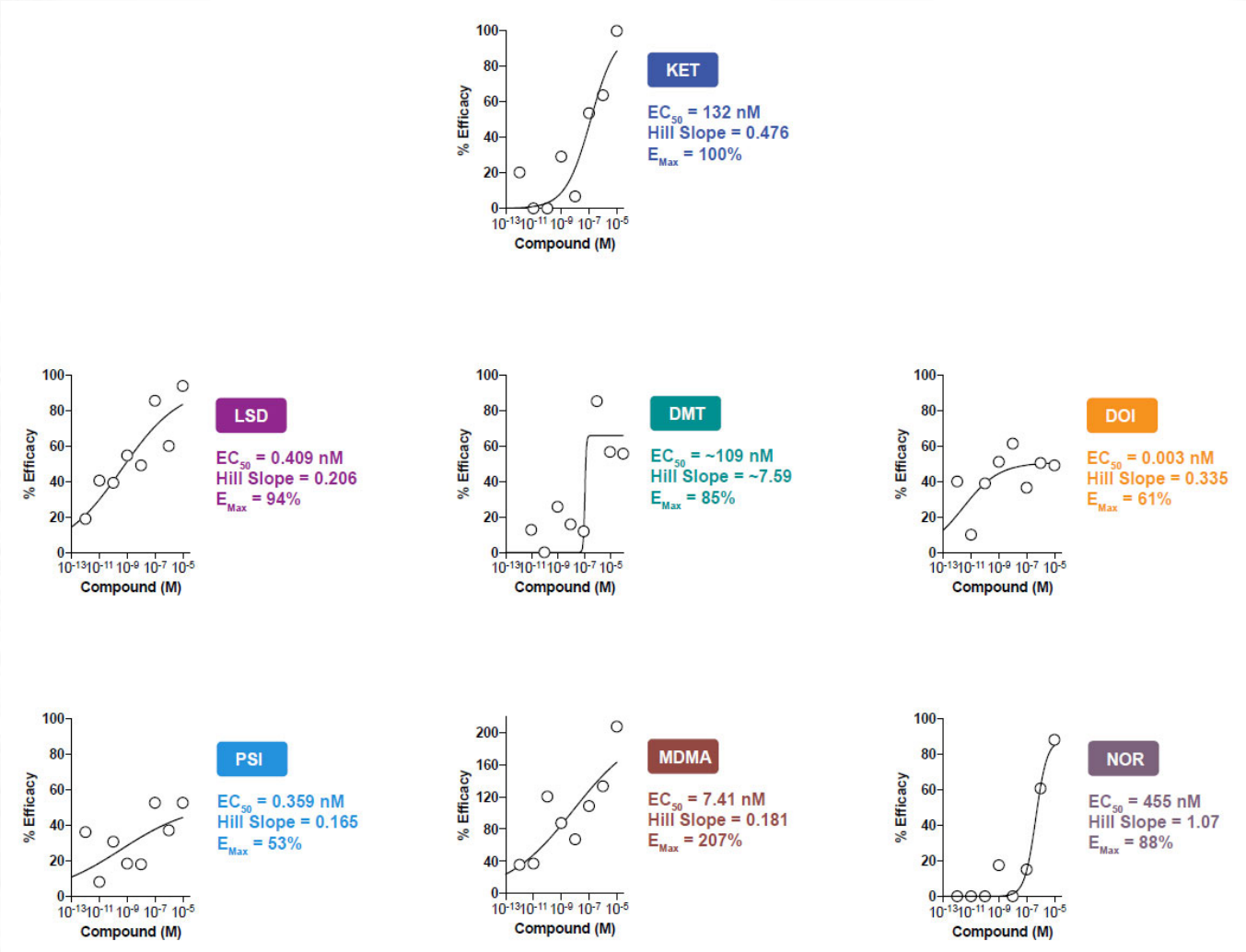

Figure S3. Psychedelics Promote Neuritogenesis in a Dose-Dependent Manner, Related to Figure 1. Cultured embryonic rat cortical neurons (DIV6) were treated with 8 decreasing concentrations of each compound (1Array-fold dilutions) and subjected to Sholl analysis. The N_{max} values obtained following treatment with 1Array µM ketamine and vehicle (Array.1% DMSO) were defined as 1ArrayArray% and Array% respectively. The maximum number of crossings (N_{max}) of the Sholl plots are reported relative to these values. Using nonlinear regression analysis, EC_{5Array} values and Hill slopes were calculated. Maximum efficacy relative to 1Array µM ketamine is also shown. Most of the compounds display Hill slopes substantially different from 1, which suggests that this cellular phenotype is not mediated by binding to a single site and implies polypharmacology. KET = ketamine, LSD = lysergic acid diethylamide, DMT = N,N-dimethyltryptamine, DOI = (±)-2,5-dimethoxy-4-iodoamphetamine, PSI = psilocin, MDMA = (±)-3,4-methylenedioxymethamphetamine, NOR = noribogaine.

Psychedelics Promote Spinogenesis and Synaptogenesis

In addition to dendritic atrophy, loss of dendritic spines is a hallmark of depression and other neuropsychiatric disorders (Christoffel *et al.*, 2011; Duman and Aghajanian, 2012), so we next assessed the effects of psychedelics on spinogenesis. We treated mature rat cortical cultures for 24 hr with DOI, DMT, and LSD as representative compounds from the amphetamine, tryptamine, and ergoline classes of psychedelics, respectively. All three compounds increased the number of dendritic spines per unit length, as measured by super-resolution structured illumination microscopy (SIM) (Figures 2A, 2B, and S6), with LSD nearly doubling the number of spines per 10 µm. Additionally, treatment caused a shift in spine morphology, favoring immature (thin and filopodium) over more mature (mushroom) spine types (Figure 2C). Colocalization of pre- and postsynaptic markers following treatment demonstrated that psychedelics promoted synaptogenesis by increasing the density, but not the size of synapses (Figure 2D-2F). This increase in synapse density was accompanied by an increase in the density of VGLUT1 puncta, but not PSD-95 puncta, following compound administration (Figures 2G and 2H).

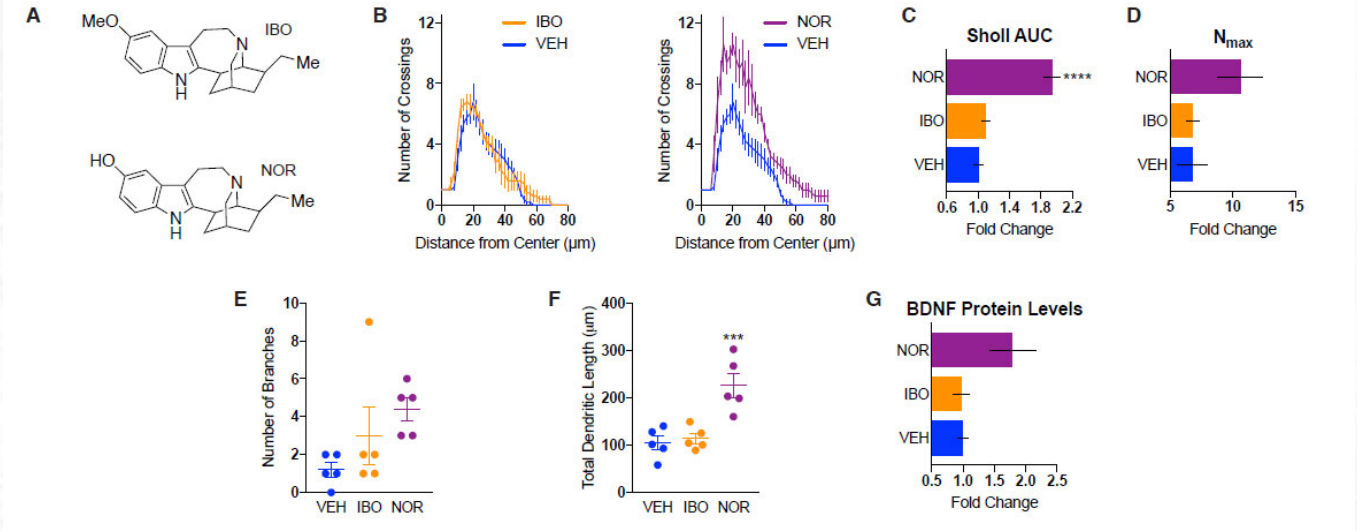

Figure S4. Noribogaine, but Not ibogaine, Promotes Structural Neural Plasticity, Related to Figure 1. (A) Chemical structures of the anti-addictive compound ibogaine and its metabolite noribogaine. (B) Sholl analysis (circle radii = 2 μm increments) demonstrates that cultured embryonic rat cortical neurons (DIV6) treated with noribogaine, but not ibogaine, have more complex dendritic arbors as compared to vehicle control (n = 5 neurons per treatment). (C) Area under the curve (AUC) of the Sholl plots in B. (D) Maximum number of crossings (N_{max}) of the Sholl plots in B. (E-F) Cultured cortical neurons treated with noribogaine, but not ibogaine, exhibited an increased number of branch points (E) and total length of the dendritic arbor (F). (G) Treatment with noribogaine, but not ibogaine, increases BDNF protein levels in DIV18 cultured cortical neurons after 24 h. Error bars represent s.e.m. *p < 0.05, **p < 0.01, ***p < 0.001, ****p < 0.0001 as compared to vehicle control (One-way ANOVA with Dunnett's post-hoc test). VEH = vehicle, IBO = Ibogaine, NOR = Noribogaine.

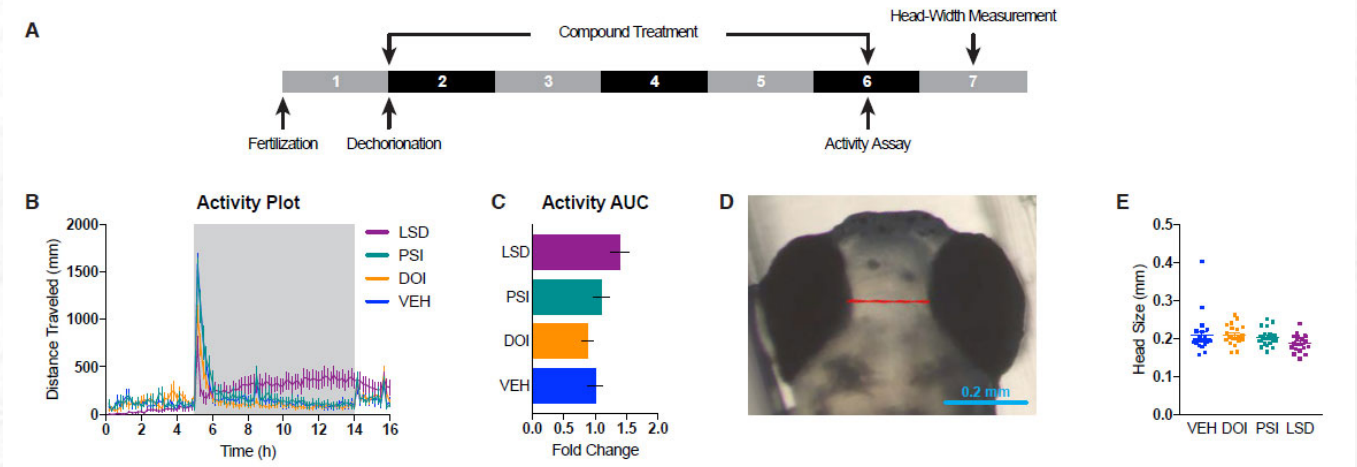

Figure S5. Psychedelics Do Not Induce Behavioral or Gross Morphological Changes in Developing Zebrafish, Related to Figure 1. (A) Experimental design used to assess the effects of psychedelics on zebrafish development. Alternating gray and black blocks represent individual days. Days are numbered in white. (B) Average activity of 5.5 dpf zebrafish (n = 23-24 zebrafish per treatment). The shaded area represents the dark period. A surge in activity immediately followed the transition from light to dark. (C) Area under the curve of the activity plot in B. (D) Representative example of a head-width measurement. (E) Treatment with psychedelics does not affect head size at 6.5 dpf. Error bars represent s.e.m. Treatments did not result in any significant differences as compared to vehicle control (One-way ANOVA with Dunnett's post-hoc test). VEH = vehicle, DOI = (±)-2,5-dimethoxy-4-iodoamphetamine, PSI = Psilocin, LSD = lysergic acid diethylamide, dpf = days post-fertilization.

Encouraged by our *in vitro* results, we next assessed the effects of a single intraperitoneal dose of DMT on spinogenesis in the PFC of adult rats using Golgi-Cox staining. We chose to administer a 10 mg/kg dose of DMT for three reasons. First, all available data suggested that this dose would produce hallucinogenic effects in rats with minimal safety risks (Glennon *et al.*, 1980, 1983; Glennon, 1999; Gatch *et al.*, 2009; Smith *et al.*, 1998; Appel *et al.*, 1999; Winter *et al.*, 2007; Carbonaro *et al.*, 2015; Helsley *et al.*, 1998; Strassman *et al.*, 1994; Nair and Jacob, 2016). Second, we have previously shown that a 10 mg/kg dose of DMT produces positive effects in rat behavioral tests relevant to depression and PTSD (Cameron *et al.*, 2018). Finally, we wanted to directly compare the effects of DMT with ketamine, and seminal studies conducted by Li *et al.* (2010) had previously demonstrated that a 10 mg/kg dose of ketamine produced a robust increase in dendritic spine density in the PFC of rats. We observed a significant increase in the density of dendritic spines on cortical pyramidal neurons 24 hr after dosing with DMT (Figures 2I and 2J). This effect was comparable with that produced by ketamine at the same dose (Figure 2J). Importantly, this DMT-induced increase in dendritic spine density was accompanied by functional effects. *Ex vivo* slice recordings revealed that both the frequency and amplitude of spontaneous excitatory postsynaptic currents (EPSCs) were increased following DMT

treatment (Figures 2K-2M). Interestingly, 10 mg/kg and 1 mg/kg doses produced similar responses despite the fact that they are predicted to be hallucinogenic and subhallucinogenic, respectively (Strassman *et al*., 1994; Nair and Jacob, 2016).

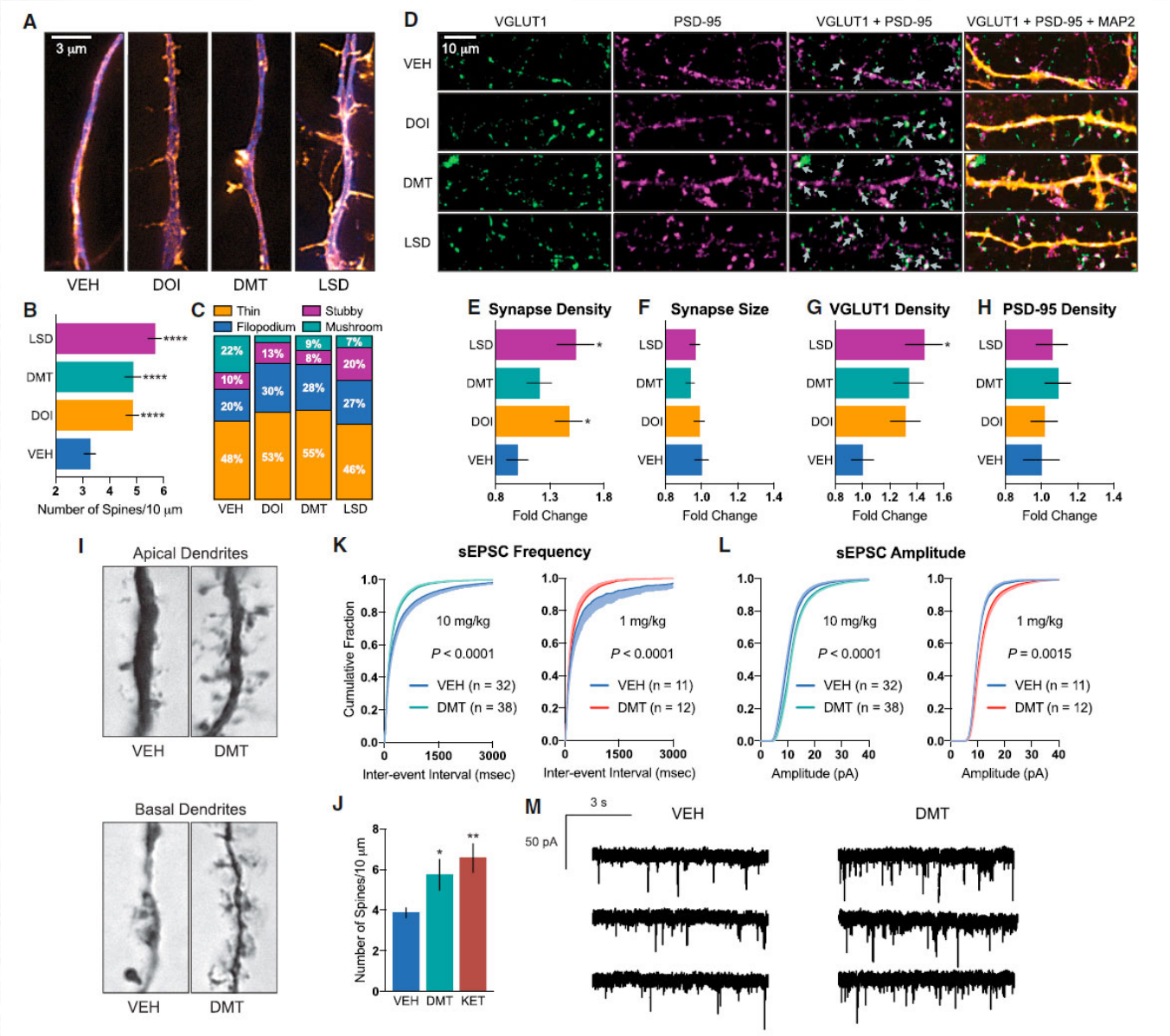

Figure 2. Psychedelics Promote Spinogenesis, Synaptogenesis, and Functional Plasticity
(A) Representative images of cortical neurons (DIV19) treated with compounds for 24 hr, demonstrating that psychedelics increase the number of dendritic spines (blue, MAP2; orange, F-actin).
(B) Quantification of spine density (n = 56-65 neurons).
(C) Relative proportions of spine types following treatment of cortical cultures with psychedelics (n = 16-21 neurons).
(D) Representative images of cortical neurons (DIV19) treated for 24 hr, demonstrating that psychedelics increase synaptogenesis (green, VGLUT1; magenta, PSD-95; yellow, MAP2). White areas in the VGLUT1 + PSD-95 images indicate colocalization of pre- and postsynaptic makers and are indicated by gray arrows.
(E-H) Quantification of synapse density (E), synapse size (F), presynaptic density (VGLUT1) (G), and postsynaptic density (PSD-95) (H) following 24-hr treatment of cortical neurons (DIV19) (n = 39-42 neurons).
(I) Representative images of Golgi-Cox-stained pyramidal neurons from the PFC of rats 24 hr after receiving a 10 mg/kg dose of DMT.
(J) Quantification of spines from (I), demonstrating that DMT (10 mg/kg) increases spinogenesis *in vivo* to a comparable extent as ketamine (10 mg/kg) (n = 11-17 neurons).
(K and L) Whole-cell voltage-clamp recordings of layer V pyramidal neurons from slices obtained 24 hr after DMT treatment (10 mg/kg and 1 mg/kg) demonstrate that DMT increases both spontaneous excitatory postsynaptic current (sEPSC) frequency (K) and amplitude (L) (n = 11-38 neurons from 3 animals).
(M) Representative traces for the 10 mg/kg experiments quantified in (K) and (L). *p < 0.05, **p < 0.01, ***p < 0.001, ****p < 0.0001, as compared to vehicle control (VEH). Data are represented as mean ± SEM. See also Figure S6.

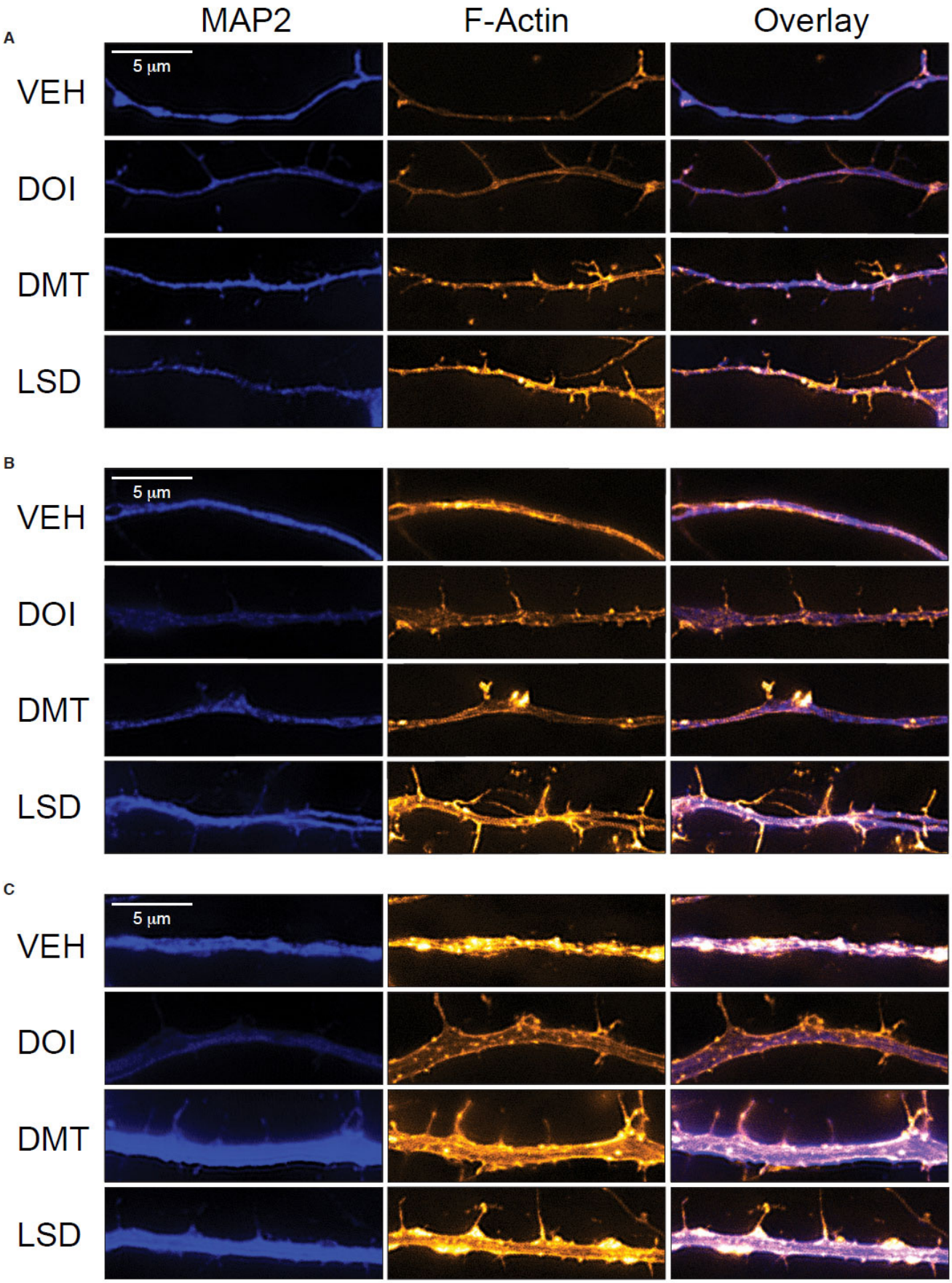

Figure S6. Psychedelics Promote Spinogenesis in Cultured Cortical Neurons, Related to Figure 2. (A-C) Representative super-resolution structured illumination microscopy (SIM) images of cultured embryonic rat cortical neurons (DIV19) treated with compounds for 24 h demonstrate that psychedelics promote spinogenesis (Blue = MAP2, Orange = F-actin). As MAP2 primarily labels the dendritic shaft while F-actin is found in all processes, orange protrusions from the shaft with minimal co-staining indicate dendritic spines. Examples of thin (A), medium (B), and thick (C) dendrites are presented.

Because the half-life of DMT is exceedingly short (~15 min), these results confirm that structural and functional changes induced by DMT persist for hours after the compound has been cleared from the body. Moreover, they demonstrate that DMT produces functional effects on pyramidal neurons of the PFC that mirror those produced by ketamine (Li *et al*., 2010). Because the PFC is a key brain region involved in extinction learning (Quirk *et al*., 2006), and both ketamine and DMT have been shown to facilitate fear extinction (Cameron *et al*., 2018; Girgenti *et al*., 2017), our results suggest a link between the plasticity-promoting and behavioral effects of these drugs. Because fear extinction can be enhanced by increasing levels of brain-derived neurotrophic factor (BDNF) in the PFC (Peters *et al*., 2010), and ketamine's behavioral effects have been shown to be BDNF-dependent (Lepack *et al*., 2014), we next sought to determine the role of BDNF signaling in the plasticity-promoting effects of classical psychedelics.

Psychedelics Promote Plasticity through a TrkBand mTOR-Dependent Mechanism

The role of BDNF in both neuritogenesis and spinogenesis is well known (Cohen-Cory *et al*., 2010), and several reports suggest that psychedelics are capable of increasing levels of neurotrophic factors (He *et al*., 2005; Martin *et al*., 2014; Nichols and Sanders-Bush, 2002; Vaidya *et al*., 1997). Therefore, we treated cortical neurons with BDNF, DOI, and a combination of the two to see whether they had any additive or synergistic effects. Dose-response studies using recombinant BDNF (Figures 3A-3C) revealed that a 50 ng/mL treatment increased neuritogenesis to a comparable extent as DOI (10 µM). Moreover, a combination of the two did not confer any added benefit, suggesting that they operate through a related mechanism (Figures 3D-3F). Next, we treated cortical neurons with DOI, DMT, and LSD for 24 hr before measuring BDNF gene and protein expression using droplet digital PCR (ddPCR) and ELISA, respectively. Although psychedelics did not increase the expression of *BDNF* transcript (Figure 3G), they did result in a 2-fold increase in BDNF protein levels, although this effect was not statistically significant (Figure 3H). When cortical cultures were co-treated with ANA-12 (Cazorla *et al*., 2011), a selective antagonist of BDNF's high-affinity receptor TrkB, the ability of psychedelics or BDNF to stimulate neuritogenesis and spinogenesis was completely blocked (Figure 4).

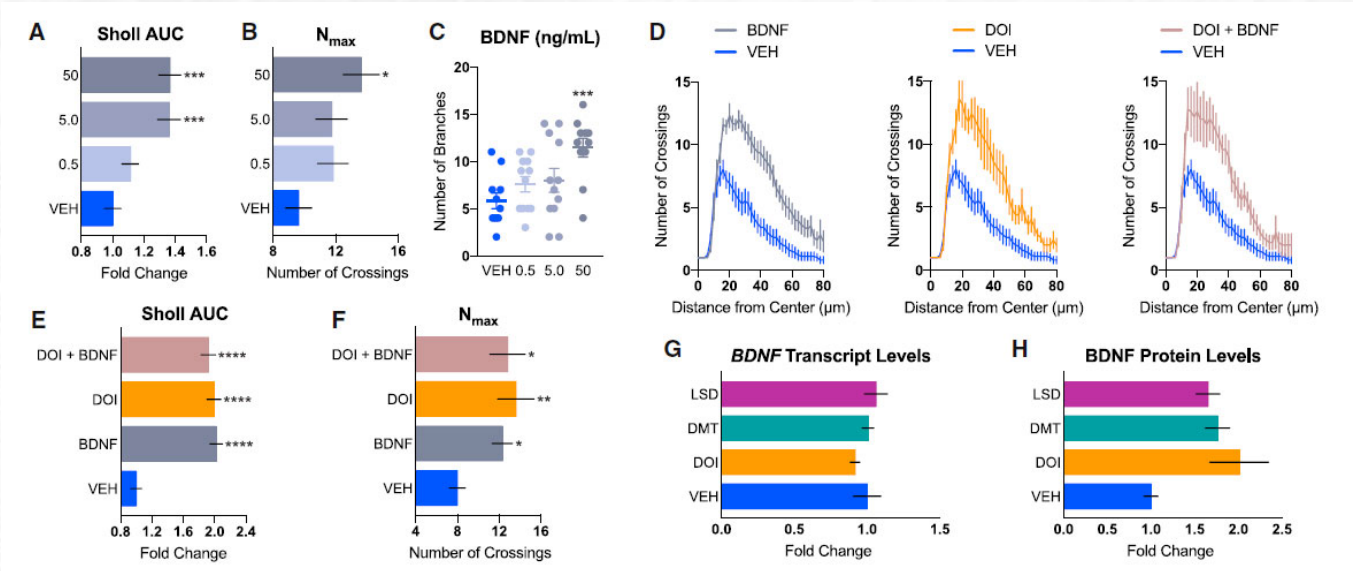

Figure 3. Psychedelics and BDNF Promote Neuritogenesis via a Related Mechanism
(A-C) Dose response of recombinant BDNF on neuritogenesis. AUC of the Sholl plots (A), N_{max} of the Sholl plots (B), and total number of branches (C) of treated cortical neurons (n = 11-12 neurons per treatment, DIV6) indicate that the highest concentration of BDNF (50 ng/mL) is more effective at promoting neuritogenesis than lower concentrations (5.0 and 0.5 ng/mL).
(D) Sholl analysis (n = 5-10 neurons) demonstrating that DOI (10 µM) increases neuritogenesis to a comparable extent as recombinant BDNF (50 ng/mL). A combination of DOI (10 µM) and BDNF (50 ng/mL) did not have any additive or synergistic effects.
(E) AUC of the Sholl plots in (D).
(F) N_{max} of the Sholl plots in (D).
(G and H) Cultured cortical neurons (DIV18) were treated with compounds for 24 hr, and then BDNF gene (G) and protein (H) expression was assessed via ddPCR (n = 4) and ELISA (n = 3-4), respectively. *p < 0.05, **p < 0.01, ***p < 0.001, ****p < 0.0001, as compared to vehicle control (VEH). Data are represented as mean ± SEM.

Activation of TrkB is known to promote signaling through mTOR (Takei *et al*., 2004), which plays a key role in structural plasticity (Jaworski *et al*., 2005; Kumar *et al*., 2005), the production of proteins necessary for

synaptogenesis (Hoeffer and Klann, 2010), and the effects of ketamine (Dwyer and Duman, 2013; Li *et al.*, 2010). Treatment with rapamycin, an mTOR inhibitor, completely blocked psychedelic-induced neuritogenesis (Figure 5), thus confirming that mTOR activation plays a role in the plasticity-promoting effects of classical serotonergic psychedelics.

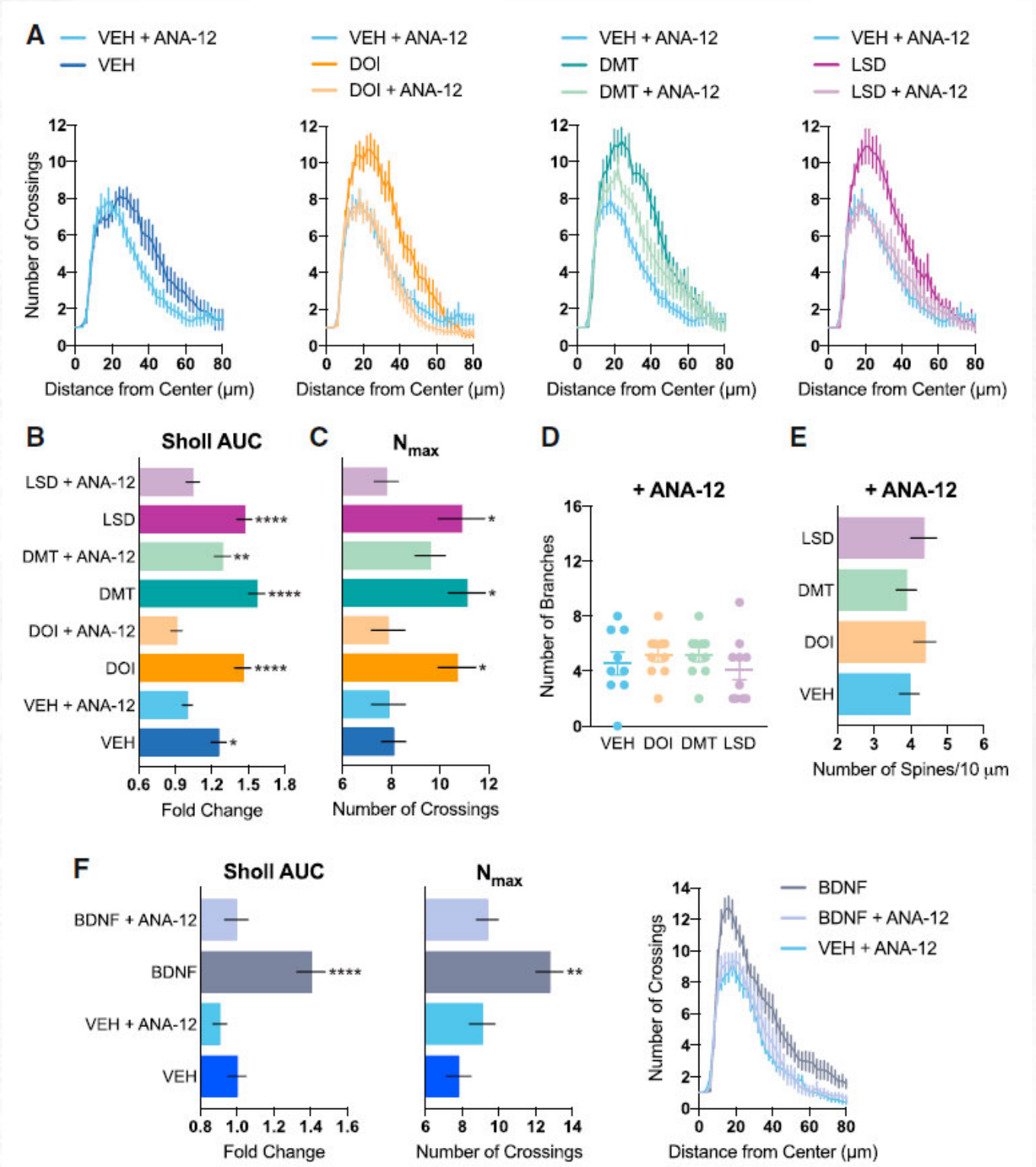

Figure 4. Psychedelic-Induced Changes in Neuronal Structure Are Mediated by TrkB
(A-D) The effects of psychedelics on dendritic arbor complexity are blocked by ANA-12, a selective inhibitor of TrkB, as measured by Sholl analysis of cultured cortical neurons (A) (DIV6). Compound-induced increases in the AUC of the Sholl plots (B), the N_{max} of the Sholl plots (C), and the number of dendritic branches (D) are completely blocked by ANA-12 (n = 8-10 neurons).
(E) The spinogenesis-promoting properties of psychedelics are blocked by ANA-12 (n = 19-21 neurons, DIV19).
(F) Control experiment demonstrating that ANA-12 blocks the effects of BDNF on neuritogenesis (n = 11-15 neurons). *$p < 0.05$, **$p < 0.01$, ***$p < 0.001$, ****$p < 0.0001$, as compared to vehicle control (VEH) or vehicle + antagonist. Data are represented as mean ± SEM.

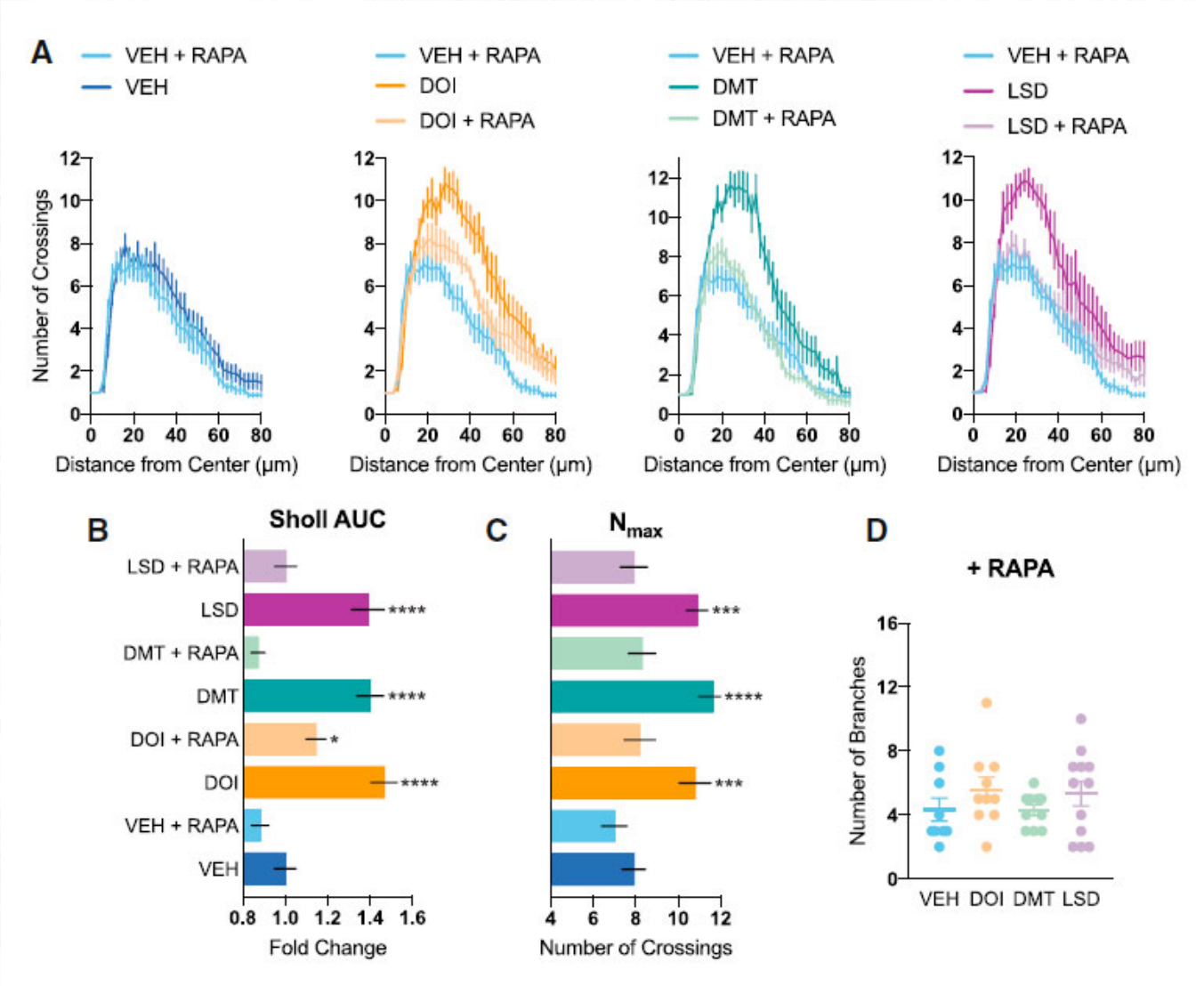

Figure 5. Psychedelic-Induced Changes in Neuronal Structure Are Mediated by mTOR
(A-D) The effects of psychedelics on dendritic arbor complexity are blocked by rapamycin, an inhibitor of mTOR, as measured by Sholl analysis of cultured cortical neurons (A) (DIV6). Compoundinduced increases in the AUC of the Sholl plots (B), the N_{max} of the Sholl plots (C), and the number of dendritic branches (D) are completely blocked by rapamycin (n = 9-12 neurons). *$p < 0.05$, **$p < 0.01$, ***$p < 0.001$, ****$p < 0.0001$, as compared to vehicle control (VEH) or vehicle + antagonist. Data are represented as mean ± SEM.

The 5-HT2A Receptor Mediates the Effects of Psychedelics on Structural Plasticity

Finally, we sought to determine whether the 5-HT_{2A} receptor played any role in the plasticity-promoting effects of DOI, DMT, and LSD because this receptor is known to be primarily responsible for the hallucinogenic effects of classical psychedelics (Nichols, 2004, 2016). Furthermore, the psychoplastogenic potencies of these and related compounds correlate well with their 5-HT_{2A} receptor affinities (Figure S3) (i.e., a higher 5-HT_{2A} binding affinity generally predicts more potent psychoplastogenic effects). Control experiments demonstrated that 5-HT_{2A} receptors were expressed on cultured rat cortical neurons at both 6 days *in vitro* (DIV6) and DIV19 (Figure 6A). Next we found that co-treatment with ketanserin, a selective 5-HT_{2A} antagonist, completely abrogated the ability of DMT, LSD, and DOI to promote both neuritogenesis and spinogenesis (Figures 6B-6F). Ketanserin was also able to block the effects of psilocin as well as the non-classical psychedelic noribogaine and entactogen MDMA (Figure 6G).

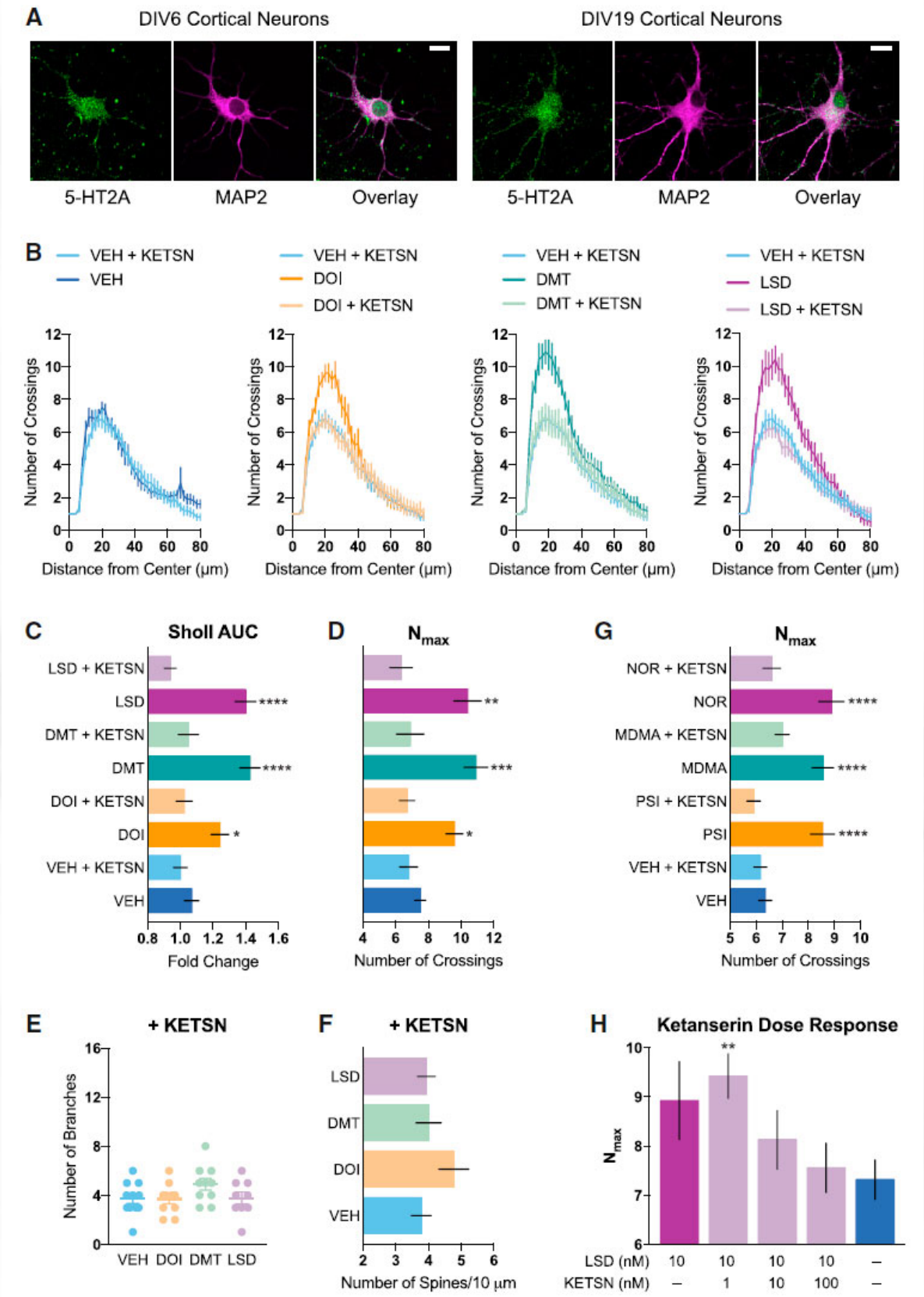

Figure 6. The 5-HT$_{2A}$ Receptor Mediates the Effects of Psychedelics on Structural Plasticity

(A) Rat embryonic cortical neurons express 5-HT$_{2A}$ receptors at both DIV6 and DIV19 (scale bar, 10 μm).

(B) The effects of psychedelics on increasing dendritic arbor complexity are blocked by cotreating with ketanserin, a selective antagonist of 5-HT$_{2A}$ receptors, as measured by Sholl analysis of cultured cortical neurons (DIV6).

(C-E) Compound-induced increases in the AUC of the Sholl plots (C), the N_{max} of the Sholl plots (D), and the number of dendritic branches (E) are completely blocked by ketanserin (n = 10-11 neurons, DIV6).

(F) The spinogenesis-promoting properties of psychedelics are blocked by ketanserin (n = 19-20 neurons, DIV19).

(G) Ketanserin also blocks the increased N_{max} induced by psilocin, noribogaine, and MDMA.

(H) Ketanserin dose-dependently blocks the psychoplastogenic effects of 10 nM LSD (n = 9-38 neurons, DIV6). *p < 0.05, **p < 0.01, ***p < 0.001, ****p < 0.0001, as compared to vehicle control (VEH) or vehicle + antagonist. Data are represented as mean ± SEM.

These initial experiments were performed using doses of psychoplastogens that produced maximal effects on structural plasticity (circa 10 µM) in combination with a 10-fold excess of ketanserin (100 µM). At these concentrations, we could not rule out the possibility of other receptors contributing to the antagonistic effects of ketanserin. Therefore, we treated cultured cortical neurons with a significantly lower dose of LSD (10 nM) and attempted to block its ability to promote neurite outgrowth using increasing doses of ketanserin (Figure 6H). We found that ketanserin blocks the psychoplastogenic effects of LSD by ~50% when treated at 10 nM. This is consistent with the fact that the binding affinities of ketanserin and LSD for the 5-HT_{2A} receptor are roughly equivalent (low nanomolar). Increasing the concentration of ketanserin to 100 nM, 10-fold higher than the concentration of LSD used in this experiment, completely prevented LSD-induced neuritogenesis. At 100 nM, ketanserin is relatively selective for the 5-HT_{2A} receptor, although, at this concentration, we cannot rule out the possible involvement of 5-HT_{2C}, adrenergic, or histamine receptors.

As a final note, the concentration responses of most psychoplastogens had Hill slopes that deviated from 1.0 (Figure S3), implying polypharmacology. Because psychedelics have relatively high affinities for 5-HT_{2A} receptors, it is likely that the effects of psychedelics are mediated primarily through 5-HT_{2A} receptors at low concentrations and modulated by other targets at high concentrations. Interestingly, the concentration response of DMT was the only one to exhibit a Hill slope greater than 1.0, indicating some form of cooperativity.

Discussion

Classical serotonergic psychedelics are known to cause changes in mood (Griffiths *et al*., 2006, 2008, 2011) and brain function (Carhart-Harris *et al*., 2017) that persist long after the acute effects of the drugs have subsided. Moreover, several psychedelics elevate glutamate levels in the cortex (Nichols, 2004, 2016) and increase gene expression *in vivo* of the neurotrophin *BDNF* as well as immediate-early genes associated with plasticity (Martin *et al*., 2014; Nichols and Sanders-Bush, 2002; Vaidya *et al*., 1997). This indirect evidence has led to the reasonable hypothesis that psychedelics promote structural and functional neural plasticity, although this assumption had never been rigorously tested (Bogenschutz and Pommy, 2012; Vollenweider and Kometer, 2010). The data presented here provide direct evidence for this hypothesis, demonstrating that psychedelics cause both structural and functional changes in cortical neurons.

Prior to this study, two reports suggested that psychedelics might be able to produce changes in neuronal structure. Jones *et al*. (2009) demonstrated that DOI was capable of transiently increasing the size of dendritic spines on cortical neurons, but no change in spine density was observed. The second study showed that DOI promoted neurite extension in a cell line of neuronal lineage (Marinova *et al*., 2017). Both of these reports utilized DOI, a psychedelic of the amphetamine class. Here we demonstrate that the ability to change neuronal structure is not a unique property of amphetamines like DOI because psychedelics from the ergoline, tryptamine, and iboga classes of compounds also promote structural plasticity. Additionally, D-amphetamine does not increase the complexity of cortical dendritic arbors in culture, and therefore, these morphological changes cannot be simply attributed to an increase in monoamine neurotransmission.

The identification of psychoplastogens belonging to distinct chemical families is an important aspect of this work because it suggests that ketamine is not unique in its ability to promote structural and functional plasticity. In addition to ketamine, the prototypical psychoplastogen, only a relatively small number of plasticity-promoting small molecules have been identified previously. Such compounds include the *N*-methyl-D-aspartate (NMDA) receptor ligand GLYX-13 (i.e., rapastinel), the mGlu2/3 antagonist LY341495, the TrkB agonist 7,8-DHF, and the muscarinic receptor antagonist scopolamine (Lepack *et al*., 2016; Castello *et al*., 2014; Zeng *et al*., 2012; Voleti *et al*., 2013). We observe that hallucinogens from four distinct structural classes (i.e., tryptamine, amphetamine, ergoline, and iboga) are also potent psychoplastogens, providing additional lead scaffolds for medicinal chemistry efforts aimed at identifying neurotherapeutics. Furthermore, our cellular assays revealed that several of these compounds were more efficacious (e.g., MDMA) or more potent (e.g., LSD) than ketamine. In fact, the plasticity-promoting properties of psychedelics and entactogens rivaled that of BDNF (Figures 3A-3C and S3). The extreme potency of LSD in particular might be due to slow off kinetics, as recently proposed following the disclosure of the LSD-bound 5-HT_{2B} crystal structure (Wacker *et al*., 2017).

Importantly, the psychoplastogenic effects of psychedelics in cortical cultures were also observed *in vivo* using both vertebrate and invertebrate models, demonstrating that they act through an evolutionarily conserved mechanism. Furthermore, the concentrations of psychedelics utilized in our *in vitro* cell culture assays were consistent with those reached in the brain following systemic administration of therapeutic doses in rodents (Yang *et al*., 2018; Cohen and Vogel, 1972). This suggests that neuritogenesis, spinogenesis, and/or synaptogenesis assays performed using cortical cultures might have value for identifying psychoplastogens and fast-acting antidepressants. It should be noted that our structural plasticity studies performed *in vitro* utilized neurons exposed to psychedelics for extended periods of time. Because brain exposure to these compounds is often of short duration due to rapid metabolism, it will be interesting to assess the kinetics of psychedelic-induced plasticity.

A key question in the field of psychedelic medicine has been whether or not psychedelics promote changes in the density of dendritic spines (Kyzar *et al*., 2017). Using super-resolution SIM, we clearly demonstrate that psychedelics do, in fact, increase the density of dendritic spines on cortical neurons, an effect that is not restricted to a particular structural class of compounds. Using DMT, we verified that cortical neuron spine density increases *in vivo* and that these changes in structural plasticity are accompanied by functional effects such as increased amplitude and frequency of spontaneous EPSCs. We specifically designed these experiments to mimic previous studies of ketamine (Li *et al*., 2010) so that we might directly compare these two compounds, and, to a first approximation, they appear to be remarkably similar. Not only do they both increase spine density and neuronal excitability in the cortex, they seem to have similar behavioral effects. We have shown previously that, like ketamine, DMT promotes fear extinction learning and has antidepressant effects in the forced swim test (Cameron *et al*., 2018). These results, coupled with the fact that ayahuasca, a DMT-containing concoction, has potent antidepressant effects in humans (Osório *et al*., 2015; Sanches *et al*., 2016; Santos *et al*., 2007), suggests that classical psychedelics and ketamine might share a related therapeutic mechanism.

Although the molecular targets of ketamine and psychedelics are different (NMDA and 5-HT_{2A} receptors, respectively), they appear to cause similar downstream effects on structural plasticity by activating mTOR. This finding is significant because ketamine is known to be addictive whereas many classical psychedelics are not (Nutt *et al*., 2007, 2010). The exact mechanisms by which these compounds stimulate mTOR is still not entirely understood, but our data suggest that, at least for classical psychedelics, TrkB and 5-HT_{2A} receptors are involved. Although most classical psychedelics are not considered to be addictive, there are still significant safety concerns with their use in medicine because they cause profound perceptual disturbances and still have the potential to be abused. Therefore, the identification of non-hallucinogenic analogs capable of promoting plasticity in the PFC could facilitate a paradigm shift in our approach to treating neuropsychiatric diseases. Moreover, such compounds could be critical to resolving the long-standing debate in the field concerning whether the subjective effects of psychedelics are necessary for their therapeutic effects (Majić *et al*., 2015). Although our group is actively investigating the psychoplastogenic properties of non-hallucinogenic analogs of psychedelics, others have reported the therapeutic potential of safer structural and functional analogs of ketamine (Moskal *et al*., 2017; Yang *et al*., 2015; Zanos *et al*., 2016).

Our data demonstrate that classical psychedelics from several distinct chemical classes are capable of robustly promoting the growth of both neurites and dendritic spines *in vitro*, *in vivo*, and across species. Importantly, our studies highlight the similarities between the effects of ketamine and those of classical serotonergic psychedelics, supporting the hypothesis that the clinical antidepressant and anxiolytic effects of these molecules might result from their ability to promote structural and functional plasticity in prefrontal cortical neurons. We have demonstrated that the plasticity-promoting properties of psychedelics require TrkB, mTOR, and 5-HT_{2A} signaling, suggesting that these key signaling hubs may serve as potential targets for the development of psychoplastogens, fast-acting antidepressants, and anxiolytics. Taken together, our results suggest that psychedelics may be used as lead structures to identify next-generation neurotherapeutics with improved efficacy and safety profiles.

Experimental Procedures

Drugs

For *in vitro* studies, all compounds were dissolved in DMSO and diluted 1:1,000, with the exception that BDNF was dissolved in water. Cells were treated with DMT at a final concentration of 90 µM (0.1% DMSO), whereas all other compounds were used at 10 µM (0.1% DMSO) unless noted otherwise. For *in vivo* studies, DMT or ketamine was dissolved in sterile 0.9% saline and administered intraperitoneally at a dose of 10 mg/kg and an injection volume of 1 mL/kg.

Animals

Sprague-Dawley rats were obtained from Charles River Laboratories (Wilmington, MA, USA). The age and sex of the animals used are noted under each individual experimental subheading. All experimental procedures involving animals were approved by the University of California, Davis Institutional Animal Care and Use Committee (IACUC) and adhered to the principles described in the NIH Guide for the Care and Use of Laboratory Animals. The University of California, Davis is accredited by the Association for Assessment and Accreditation of Laboratory Animal Care International (AAALAC) and has an Animal Welfare Assurance number (A3433-01) on file with the Office of Laboratory Animal Welfare (OLAW).

Cell Culture

Primary cortical cultures were prepared using tissue from embryonic day 18 (E18) Sprague-Dawley rats. Cells were plated at various densities on poly-Dlysine-coated plates depending on the specific experiment (Supplemental Experimental Procedures). Plating medium consisted of 10% heat-inactivated fetal bovine serum (FBS) (Life Technologies), 1% penicillin-streptomycin (Life Technologies), and 0.5 mM glutamine (Life Technologies) in Neurobasal (Life Technologies). After 15-24 hr, the medium was removed and exchanged for replacement medium containing 13 B27 supplement (Life Technologies), 1% penicillin-streptomycin, 0.5 mM glutamine, 12.5 µM glutamate, and Neurobasal. After 96 hr, 50% of the medium was removed and replaced with feed medium containing 13 B27 supplement, 1% penicillin-streptomycin, and 0.5 mM glutamine. Once per week, until the cultures had reached sufficient maturity for experiments, 50% of the culture medium was removed and replaced with feed medium, with an additional 20% by volume being added to account for evaporation. For experiments using antagonists or inhibitors, cells were pretreated with ANA-12 (10 µM), rapamycin (100 nM), and ketanserin (100 µM) for 10 min prior to addition of test compounds unless otherwise noted. The final DMSO concentration of these experiments was 0.2%. The neurons used in each cellular experiment were taken from at least two different treatment wells, and the wells were randomized to account for plate effects. All of the cellular experiments were replicated on at least two occasions by two or more experimenters.

Statistical Analysis

Appropriate samples sizes were estimated based on our previous experiences performing similar experiments. Data are represented as mean ± SEM. Statistical analyses were performed using GraphPad Prism (version 7.0a). For analyses involving comparison of three or more groups, a one-way analysis of variance (Dunnett's *post hoc* test) was utilized. No statistics were calculated for the individual points of the Sholl plots. Instead, statistical analyses were performed on the aggregate data (i.e., the area under the curve of the Sholl plot). Probability distributions from electrophysiology experiments were compared using a Kolmogorov-Smirnov test. *$p < 0.05$, **$p < 0.01$, ***$p < 0.001$, and ****$p < 0.0001$ compared with vehicle control or vehicle + antagonist.

Acknowledgments

We thank Lee E. Dunlap for synthesizing DMT, Aurora Martinez-Horta for assistance with Golgi-Cox staining experiments, the Light Microscopy Imaging Facility in the Department of Molecular and Cellular Biology for the use of their Nikon N-SIM, Javier González-Maeso for providing 198A2 cells, and members of the Olson laboratory for discussions regarding the manuscript. We also thank Valentina Popescu in the Department of Classics at UC Davis for assistance with coining the term ''psychoplastogen.'' Several antibodies were generously provided by the Stanley Center for Psychiatric Research at the Broad Institute. This work was supported by funds from the UC Davis Department of Chemistry and Department of Biochemistry and Molecular Medicine, a UC Davis Provost's Undergraduate Fellowship (to A.C.G.), a UC Davis MIND Institute IDDRC grant U54 HD079125 (to M.Y.D. and K.B.), an Alfred P. Sloan Fellowship (FG-2016-6814 to M.Y.D.), and NIH grants T32GM113770 (to C.L.) and 5T32MH082174-09 (to L.P.C. and E.B.).

Author Contributions

D.E.O., C.L., and A.K.M. were responsible for the overall experimental design. C.L. performed the majority of the neuritogenesis, spinogenesis, synaptogenesis, and biochemical experiments described, with A.C.G. and S.S.Z. providing assistance. C.L., L.P.C., and D.E.O. performed the Golgi-Cox staining experiments. L.P.C., J.M.W., and E.V.B. performed the electrophysiology experiments, with J.A.G. supervising these studies. K.M.O.-M. and P.C.W. performed the experiments in *Drosophila*. M.Y.D. and K.F.B. performed the zebrafish experiments. A.S. developed the program for analyzing synapse number and size. M.R.P. supervised the SIM experiments. W.C.D. performed 5-HT_{2A} expression studies and assisted with fluorescence microscopy data analysis. D.E.O. conceived the project, supervised the experiments, and wrote the manuscript with input from all authors.

Declaration of Interests

D.E.O. has submitted a patent application related to this work (PCT/US2017/ 054277).

Received: November 16, 2017
Revised: April 3, 2018
Accepted: May 7, 2018
Published: June 12, 2018

References

1. Alper, K.R. (2001). Ibogaine: a review. Alkaloids Chem. Biol. 56, 1-38.
2. Appel, J.B., West, W.B., Rolandi, W.G., Alici, T., and Pechersky, K. (1999). Increasing the selectivity of drug discrimination procedures. Pharmacol. Biochem. Behav. 64, 353-358.
3. Arnsten, A.F.T. (2009). Stress signalling pathways that impair prefrontal cortex structure and function. Nat. Rev. Neurosci. 10, 410-422.
4. Autry, A.E., and Monteggia, L.M. (2012). Brain-derived neurotrophic factor and neuropsychiatric disorders. Pharmacol. Rev. 64, 238-258.
5. Autry, A.E., Adachi, M., Nosyreva, E., Na, E.S., Los, M.F., Cheng, P.F., Kavalali, E.T., and Monteggia, L.M. (2011). NMDA receptor blockade at rest triggers rapid behavioural antidepressant responses. Nature 475, 91-95.
6. Baumann, M.H., Pablo, J.P., Ali, S.F., Rothman, R.B., and Mash, D.C. (2000). Noribogaine (12-hydroxyibogamine): a biologically active metabolite of the antiaddictive drug ibogaine. Ann. N Y Acad. Sci. 914, 354-368.
7. Baumann, M.H., Pablo, J., Ali, S.F., Rothman, R.B., and Mash, D.C. (2001). Comparative neuropharmacology of ibogaine and its O-desmethyl metabolite, noribogaine. Alkaloids Chem. Biol. 56, 79-113.
8. Belgers, M., Leenaars, M., Homberg, J.R., Ritskes-Hoitinga, M., Schellekens, A.F., and Hooijmans, C.R. (2016). Ibogaine and addiction in the animal model, a systematic review and meta-analysis. Transl. Psychiatry 6, e826.
9. Berman, R.M., Cappiello, A., Anand, A., Oren, D.A., Heninger, G.R., Charney, D.S., and Krystal, J.H. (2000). Antidepressant effects of ketamine in depressed patients. Biol. Psychiatry 47, 351-354.
10. Bogenschutz, M.P., and Pommy, J.M. (2012). Therapeutic mechanisms of classic hallucinogens in the treatment of addictions: from indirect evidence to testable hypotheses. Drug Test. Anal. 4, 543-555.
11. Bouso, J.C., Doblin, R., Farré, M., Alcázar, M.A., and Gómez-Jarabo, G. (2008). MDMA-assisted psychotherapy using low doses in a small sample of women with chronic posttraumatic stress disorder. J. Psychoactive Drugs 40, 225-236.

12. Browne, C.A., and Lucki, I. (2013). Antidepressant effects of ketamine: mechanisms underlying fast-acting novel antidepressants. Front. Pharmacol. 4, 161.
13. Cameron, L.P., Benson, C.J., Dunlap, L.E., and Olson, D.E. (2018). Effects of *N*,*N*-dimethyltryptamine on rat behaviors relevant to anxiety and depression. ACS Chem. Neurosci. Published online April 24, 2018. https://doi.org/10.1021/acschemneuro.8b00134.
14. Carbonaro, T.M., Eshleman, A.J., Forster, M.J., Cheng, K., Rice, K.C., and Gatch, M.B. (2015). The role of 5-HT2A, 5-HT2C and mGlu2 receptors in the behavioral effects of tryptamine hallucinogens *N*,*N*-dimethyltryptamine and *N*,*N*-diisopropyltryptamine in rats and mice. Psychopharmacology (Berl.) 232, 275-284.
15. Carhart-Harris, R.L., and Goodwin, G.M. (2017). The therapeutic potential of psychedelic drugs: past, present, and future. Neuropsychopharmacology 42, 2105-2113.
16. Carhart-Harris, R.L., Bolstridge, M., Rucker, J., Day, C.M., Erritzoe, D., Kaelen, M., Bloomfield, M., Rickard, J.A., Forbes, B., Feilding, A., *et al*. (2016). Psilocybin with psychological support for treatment-resistant depression: an open-label feasibility study. Lancet Psychiatry 3, 619-627.
17. Carhart-Harris, R.L., Roseman, L., Bolstridge, M., Demetriou, L., Pannekoek, J.N., Wall, M.B., Tanner, M., Kaelen, M., McGonigle, J., Murphy, K., *et al*. (2017). Psilocybin for treatment-resistant depression: fMRI-measured brain mechanisms. Sci. Rep. 7, 13187.
18. Castello, N.A., Nguyen, M.H., Tran, J.D., Cheng, D., Green, K.N., and LaFerla, F.M. (2014). 7,8-Dihydroxyflavone, a small molecule TrkB agonist, improves spatial memory and increases thin spine density in a mouse model of Alzheimer disease-like neuronal loss. PLoS ONE 9, e91453.
19. Castrén, E., and Antila, H. (2017). Neuronal plasticity and neurotrophic factors in drug responses. Mol. Psychiatry 22, 1085-1095.
20. Catlow, B.J., Song, S., Paredes, D.A., Kirstein, C.L., and Sanchez-Ramos, J. (2013). Effects of psilocybin on hippocampal neurogenesis and extinction of trace fear conditioning. Exp. Brain Res. 228, 481-491.
21. Cazorla, M., Preémont, J., Mann, A., Girard, N., Kellendonk, C., and Rognan, D. (2011). Identification of a low-molecular weight TrkB antagonist with anxiolytic and antidepressant activity in mice. J. Clin. Invest. 121, 1846-1857.
22. Christoffel, D.J., Golden, S.A., and Russo, S.J. (2011). Structural and synaptic plasticity in stress-related disorders. Rev. Neurosci. 22, 535-549.
23. Cohen, I., and Vogel, W.H. (1972). Determination and physiological disposition of dimethyltryptamine and diethyltryptamine in rat brain, liver and plasma. Biochem. Pharmacol. 21, 1214-1216.
24. Cohen-Cory, S., Kidane, A.H., Shirkey, N.J., and Marshak, S. (2010). Brainderived neurotrophic factor and the development of structural neuronal connectivity. Dev. Neurobiol. 70, 271-288.
25. Cramer, S.C., Sur, M., Dobkin, B.H., O'Brien, C., Sanger, T.D., Trojanowski, J.Q., Rumsey, J.M., Hicks, R., Cameron, J., Chen, D., *et al*. (2011). Harnessing neuroplasticity for clinical applications. Brain 134, 1591-1609.
26. Diaz-Granados, N., Ibrahim, L.A., Brutsche, N.E., Ameli, R., Henter, I.D., Luckenbaugh, D.A., Machado-Vieira, R., and Zarate, C.A., Jr. (2010). Rapid resolution of suicidal ideation after a single infusion of an *N*-methyl-D-aspartate antagonist in patients with treatment-resistant major depressive disorder. J. Clin. Psychiatry 71, 1605-1611.
27. Dos Santos, R.G., Osoório, F.L., Crippa, J.A., Riba, J., Zuardi, A.W., and Hallak, J.E. (2016). Antidepressive, anxiolytic, and antiaddictive effects of ayahuasca, psilocybin and lysergic acid diethylamide (LSD): a systematic review of clinical trials published in the last 25 years. Ther. Adv. Psychopharmacol. 6, 193-213.
28. Duman, R.S. (2002). Synaptic plasticity and mood disorders. Mol. Psychiatry 7 (Suppl 1), S29-S34.
29. Duman, R.S., and Aghajanian, G.K. (2012). Synaptic dysfunction in depression: potential therapeutic targets. Science 338, 68-72.
30. Duman, R.S., Aghajanian, G.K., Sanacora, G., and Krystal, J.H. (2016). Synaptic plasticity and depression: new insights from stress and rapid-acting antidepressants. Nat. Med. 22, 238-249.
31. Dwyer, J.M., and Duman, R.S. (2013). Activation of mammalian target of rapamycin and synaptogenesis: role in the actions of rapid-acting antidepressants. Biol. Psychiatry 73, 1189-1198.
32. Feder, A., Parides, M.K., Murrough, J.W., Perez, A.M., Morgan, J.E., Saxena, S., Kirkwood, K., Aan Het Rot, M., Lapidus, K.A., Wan, L.B., *et al*. (2014). Efficacy of intravenous ketamine for treatment of chronic posttraumatic stress disorder: a randomized clinical trial. JAMA Psychiatry 71, 681-688.
33. Gatch, M.B., Rutledge, M.A., Carbonaro, T., and Forster, M.J. (2009). Comparison of the discriminative stimulus effects of dimethyltryptamine with different classes of psychoactive compounds in rats. Psychopharmacology (Berl.) 204, 715-724.
34. Girgenti, M.J., Ghosal, S., LoPresto, D., Taylor, J.R., and Duman, R.S. (2017). Ketamine accelerates fear extinction via mTORC1 signaling. Neurobiol. Dis. 100, 1-8.
35. Glennon, R.A. (1999). Arylalkylamine drugs of abuse: an overview of drug discrimination studies. Pharmacol. Biochem. Behav. 64, 251-256.
36. Glennon, R.A., Young, R., Rosecrans, J.A., and Kallman, M.J. (1980). Hallucinogenic agents as discriminative stimuli: a correlation with serotonin receptor affinities. Psychopharmacology (Berl.) 68, 155-158.
37. Glennon, R.A., Young, R., Jacyno, J.M., Slusher, M., and Rosecrans, J.A. (1983). DOM-stimulus generalization to LSD and other hallucinogenic indolealkylamines. Eur. J. Pharmacol. 86, 453-459.
38. Griffiths, R.R., Richards, W.A., McCann, U., and Jesse, R. (2006). Psilocybin can occasion mystical-type experiences having substantial and sustained personal meaning and spiritual significance. Psychopharmacology (Berl.) 187, 268-283, discussion 284-292.
39. Griffiths, R.R., Richards, W.A., Johnson, M., McCann, U., and Jesse, R. (2008). Mystical-type experiences occasioned by psilocybin mediate the attribution of personal meaning and spiritual significance 14 months later. J. Psychopharmacol. (Oxford) 22, 621-632.
40. Griffiths, R.R., Johnson, M.W., Richards, W.A., Richards, B.D., McCann, U., and Jesse, R. (2011). Psilocybin occasioned mystical-type experiences: immediate and persisting dose-related effects. Psychopharmacology (Berl.) 218, 649-665.
41. Grob, C.S., Danforth, A.L., Chopra, G.S., Hagerty, M., McKay, C.R., Halberstadt, A.L., and Greer, G.R. (2011). Pilot study of

psilocybin treatment for anxiety in patients with advanced-stage cancer. Arch. Gen. Psychiatry 68, 71-78.
42. Grueber, W.B., Jan, L.Y., and Jan, Y.N. (2002). Tiling of the Drosophila epidermis by multidendritic sensory neurons. Development 129, 2867-2878.
43. Gustavsson, A., Svensson, M., Jacobi, F., Allgulander, C., Alonso, J., Beghi, E., Dodel, R., Ekman, M., Faravelli, C., Fratiglioni, L., *et al*.; CDBE2010Study Group (2011). Cost of disorders of the brain in Europe 2010. Eur. Neuropsychopharmacol. 21, 718-779.
44. Hayley, S., and Litteljohn, D. (2013). Neuroplasticity and the next wave of antidepressant strategies. Front. Cell. Neurosci. 7, 218.
45. He, D.Y., McGough, N.N., Ravindranathan, A., Jeanblanc, J., Logrip, M.L., Phamluong, K., Janak, P.H., and Ron, D. (2005). Glial cell line-derived neurotrophic factor mediates the desirable actions of the anti-addiction drug ibogaine against alcohol consumption. J. Neurosci. 25, 619-628.
46. Helsley, S., Fiorella, D., Rabin, R.A., and Winter, J.C. (1998). A comparison of *N*,*N*-dimethyltryptamine, harmaline, and selected congeners in rats trained with LSD as a discriminative stimulus. Prog. Neuropsychopharmacol. Biol. Psychiatry 22, 649-663.
47. Hoeffer, C.A., and Klann, E. (2010). mTOR signaling: at the crossroads of plasticity, memory and disease. Trends Neurosci. 33, 67-75.
48. Ionescu, D.F., Swee, M.B., Pavone, K.J., Taylor, N., Akeju, O., Baer, L., Nyer, M., Cassano, P., Mischoulon, D., Alpert, J.E., *et al*. (2016). Rapid and Sustained Reductions in Current Suicidal Ideation Following Repeated Doses of Intravenous Ketamine: Secondary Analysis of an Open-Label Study. J. Clin. Psychiatry 77, e719-e725.
49. Izquierdo, A., Wellman, C.L., and Holmes, A. (2006). Brief uncontrollable stress causes dendritic retraction in infralimbic cortex and resistance to fear extinction in mice. J. Neurosci. 26, 5733-5738.
50. Jang, S.W., Liu, X., Yepes, M., Shepherd, K.R., Miller, G.W., Liu, Y., Wilson, W.D., Xiao, G., Blanchi, B., Sun, Y.E., and Ye, K. (2010). A selective TrkB agonist with potent neurotrophic activities by 7,8-dihydroxyflavone. Proc. Natl. Acad. Sci. USA 107, 2687-2692.
51. Jaworski, J., Spangler, S., Seeburg, D.P., Hoogenraad, C.C., and Sheng, M. (2005). Control of dendritic arborization by the phosphoinositide-3'-kinase-Akt-mammalian target of rapamycin pathway. J. Neurosci. 25, 11300-11312.
52. Jones, K.A., Srivastava, D.P., Allen, J.A., Strachan, R.T., Roth, B.L., and Penzes, P. (2009). Rapid modulation of spine morphology by the 5-HT2A serotonin receptor through kalirin-7 signaling. Proc. Natl. Acad. Sci. USA 106, 19575-19580.
53. Kelly, T.M., and Daley, D.C. (2013). Integrated treatment of substance use and psychiatric disorders. Soc. Work Public Health 28, 388-406.
54. Kolb, B., and Muhammad, A. (2014). Harnessing the power of neuroplasticity for intervention. Front. Hum. Neurosci. 8, 377.
55. Krupitsky, E., Burakov, A., Romanova, T., Dunaevsky, I., Strassman, R., and Grinenko, A. (2002). Ketamine psychotherapy for heroin addiction: immediate effects and two-year follow-up. J. Subst. Abuse Treat. 23, 273-283.
56. Krystal, J.H., Tolin, D.F., Sanacora, G., Castner, S.A., Williams, G.V., Aikins, D.E., Hoffman, R.E., and D'Souza, D.C. (2009). Neuroplasticity as a target for the pharmacotherapy of anxiety disorders, mood disorders, and schizophrenia. Drug Discov. Today 14, 690-697.
57. Kumar, V., Zhang, M.X., Swank, M.W., Kunz, J., and Wu, G.Y. (2005). Regulation of dendritic morphogenesis by Ras-PI3K-Akt-mTOR and Ras-MAPK signaling pathways. J. Neurosci. 25, 11288-11299.
58. Kyzar, E.J., Nichols, C.D., Gainetdinov, R.R., Nichols, D.E., and Kalueff, A.V. (2017). Psychedelic Drugs in Biomedicine. Trends Pharmacol. Sci. 38, 992-1005.
59. Lepack, A.E., Fuchikami, M., Dwyer, J.M., Banasr, M., and Duman, R.S. (2014). BDNF release is required for the behavioral actions of ketamine. Int. J. Neuropsychopharmacol. 18, pyu033.
60. Lepack, A.E., Bang, E., Lee, B., Dwyer, J.M., and Duman, R.S. (2016). Fastacting antidepressants rapidly stimulate ERK signaling and BDNF release in primary neuronal cultures. Neuropharmacology 111, 242-252.
61. Li, N., Lee, B., Liu, R.J., Banasr, M., Dwyer, J.M., Iwata, M., Li, X.Y., Aghajanian, G., and Duman, R.S. (2010). mTOR-dependent synapse formation underlies the rapid antidepressant effects of NMDA antagonists. Science 329, 959-964.
62. Majic, T., Schmidt, T.T., and Gallinat, J. (2015). Peak experiences and the afterglow phenomenon: when and how do therapeutic effects of hallucinogens depend on psychedelic experiences? J. Psychopharmacol. (Oxford) 29, 241-253.
63. Marinova, Z., Walitza, S., and Grunblatt, E. (2017). The hallucinogen 2,5-dimethoxy-4-iodoamphetamine hydrochloride activates neurotrophin receptors in a neuronal cell line and promotes neurites extension. J. Neural Transm. (Vienna) 124, 749-759.
64. Martin, D.A., Marona-Lewicka, D., Nichols, D.E., and Nichols, C.D. (2014). Chronic LSD alters gene expression profiles in the mPFC relevant to schizophrenia. Neuropharmacology 83, 1-8.
65. Mathew, S.J., Manji, H.K., and Charney, D.S. (2008). Novel drugs and therapeutic targets for severe mood disorders. Neuropsychopharmacology 33, 2080-2092.
66. Mithoefer, M.C., Wagner, M.T., Mithoefer, A.T., Jerome, L., and Doblin, R. (2011). The safety and efficacy of +/-3,4-methylenedioxymethamphetamineassisted psychotherapy in subjects with chronic, treatment-resistant posttraumatic stress disorder: the first randomized controlled pilot study. J. Psychopharmacol. (Oxford) 25, 439-452.
67. Mithoefer, M.C., Wagner, M.T., Mithoefer, A.T., Jerome, L., Martin, S.F., Yazar-Klosinski, B., Michel, Y., Brewerton, T.D., and Doblin, R. (2013). Durability of improvement in post-traumatic stress disorder symptoms and absence of harmful effects or drug dependency after 3,4-methylenedioxymethamphetamine-assisted psychotherapy: a prospective long-term follow-up study. J. Psychopharmacol. (Oxford) 27, 28-39.
68. Mithoefer, M.C., Grob, C.S., and Brewerton, T.D. (2016). Novel psychopharmacological therapies for psychiatric disorders: psilocybin and MDMA. Lancet Psychiatry 3, 481-488.
69. Moskal, J.R., Burgdorf, J.S., Stanton, P.K., Kroes, R.A., Disterhoft, J.F., Burch, R.M., and Khan, M.A. (2017). The development of rapastinel (formerly GLYX-13); a rapid acting and long lasting antidepressant. Curr. Neuropharmacol. 15, 47-56.
70. Murrough, J.W., Perez, A.M., Pillemer, S., Stern, J., Parides, M.K., aan het Rot, M., Collins, K.A., Mathew, S.J., Charney, D.S., and Iosifescu, D.V. (2013). Rapid and longer-term antidepressant effects of repeated ketamine infusions in treatment-resistant

major depression. Biol. Psychiatry 74, 250-256.
71. Nair, A.B., and Jacob, S. (2016). A simple practice guide for dose conversion between animals and human. J. Basic Clin. Pharm. 7, 27-31.
72. Nichols, D.E. (2004). Hallucinogens. Pharmacol. Ther. 101, 131-181.
73. Nichols, D.E. (2016). Psychedelics. Pharmacol. Rev. 68, 264-355.
74. Nichols, C.D., and Sanders-Bush, E. (2002). A single dose of lysergic acid diethylamide influences gene expression patterns within the mammalian brain. Neuropsychopharmacology 26, 634-642.
75. Nichols, D.E., Johnson, M.W., and Nichols, C.D. (2017). Psychedelics as medicines: an emerging new paradigm. Clin. Pharmacol. Ther. 101, 209-219.
76. Nutt, D., King, L.A., Saulsbury, W., and Blakemore, C. (2007). Development of a rational scale to assess the harm of drugs of potential misuse. Lancet 369, 1047-1053.
77. Nutt, D.J., King, L.A., and Phillips, L.D.; Independent Scientific Committee on Drugs (2010). Drug harms in the UK: a multicriteria decision analysis. Lancet 376, 1558-1565.
78. Oehen, P., Traber, R., Widmer, V., and Schnyder, U. (2013). A randomized, controlled pilot study of MDMA (± 3,4-Methylenedioxymethamphetamine)-assisted psychotherapy for treatment of resistant, chronic Post-Traumatic Stress Disorder (PTSD). J. Psychopharmacol. (Oxford) 27, 40-52.
79. Osório, Fde.L., Sanches, R.F., Macedo, L.R., Santos, R.G., Maia-de-Oliveira, J.P., Wichert-Ana, L., Araujo, D.B., Riba, J., Crippa, J.A., and Hallak, J.E. (2015). Antidepressant effects of a single dose of ayahuasca in patients with recurrent depression: a preliminary report. Rev. Bras. Psiquiatr. 37, 13-20.
80. Peters, J., Dieppa-Perea, L.M., Melendez, L.M., and Quirk, G.J. (2010). Induction of fear extinction with hippocampal-infralimbic BDNF. Science 328, 1288-1290.
81. Pittenger, C., and Duman, R.S. (2008). Stress, depression, and neuroplasticity: a convergence of mechanisms. Neuropsychopharmacology 33, 88-109.
82. Qiao, H., Li, M.X., Xu, C., Chen, H.B., An, S.C., and Ma, X.M. (2016). Dendritic Spines in Depression: What We Learned from Animal Models. Neural Plast. 2016, 8056370.
83. Quirk, G.J., Garcia, R., and González-Lima, F. (2006). Prefrontal mechanisms in extinction of conditioned fear. Biol. Psychiatry 60, 337-343.
84. Ristanović, D., Milosević, N.T., and Stulić, V. (2006). Application of modified Sholl analysis to neuronal dendritic arborization of the cat spinal cord. J. Neurosci. Methods 158, 212-218.
85. Rucker, J.J., Jelen, L.A., Flynn, S., Frowde, K.D., and Young, A.H. (2016). Psychedelics in the treatment of unipolar mood disorders: a systematic review. J. Psychopharmacol. (Oxford) 30, 1220-1229.
86. Rush, A.J., Trivedi, M.H., Wiśniewski, S.R., Nierenberg, A.A., Stewart, J.W., Warden, D., Niederehe, G., Thase, M.E., Lavori, P.W., Lebowitz, B.D., *et al*. (2006). Acute and longer-term outcomes in depressed outpatients requiring one or several treatment steps: a STAR*D report. Am. J. Psychiatry 163, 1905-1917.
87. Russo, S.J., and Nestler, E.J. (2013). The brain reward circuitry in mood disorders. Nat. Rev. Neurosci. 14, 609-625.
88. Russo, S.J., Mazei-Robison, M.S., Ables, J.L., and Nestler, E.J. (2009). Neurotrophic factors and structural plasticity in addiction. Neuropharmacology 56 (Suppl 1), 73-82.
89. Sanches, R.F., de Lima Osório, F., Dos Santos, R.G., Macedo, L.R., Maia-deOliveira, J.P., Wichert-Ana, L., de Araujo, D.B., Riba, J., Crippa, J.A., and Hallak, J.E. (2016). Antidepressant effects of a single dose of ayahuasca in patients with recurrent depression: a SPECT study. J. Clin. Psychopharmacol. 36, 77-81.
90. Santos, R.G., Landeira-Fernandez, J., Strassman, R.J., Motta, V., and Cruz, A.P. (2007). Effects of ayahuasca on psychometric measures of anxiety, panic-like and hopelessness in Santo Daime members. J. Ethnopharmacol. 112, 507-513.
91. Smith, R.L., Canton, H., Barrett, R.J., and Sanders-Bush, E. (1998). Agonist properties of *N,N*-dimethyltryptamine at serotonin 5-HT2A and 5-HT2C receptors. Pharmacol. Biochem. Behav. 61, 323-330.
92. Strassman, R.J., Qualls, C.R., Uhlenhuth, E.H., and Kellner, R. (1994). Doseresponse study of *N,N*-dimethyltryptamine in humans. II. Subjective effects and preliminary results of a new rating scale. Arch. Gen. Psychiatry 51, 98-108.
93. Takei, N., Inamura, N., Kawamura, M., Namba, H., Hara, K., Yonezawa, K., and Nawa, H. (2004). Brain-derived neurotrophic factor induces mammalian target of rapamycin-dependent local activation of translation machinery and protein synthesis in neuronal dendrites. J. Neurosci. 24, 9760-9769.
94. Vaidya, V.A., Marek, G.J., Aghajanian, G.K., and Duman, R.S. (1997). 5-HT_{2A} receptor-mediated regulation of brain-derived neurotrophic factor mRNA in the hippocampus and the neocortex. J. Neurosci. 17, 2785-2795.
95. Voleti, B., Navarria, A., Liu, R.J., Banasr, M., Li, N., Terwilliger, R., Sanacora, G., Eid, T., Aghajanian, G., and Duman, R.S. (2013). Scopolamine rapidly increases mammalian target of rapamycin complex 1 signaling, synaptogenesis, and antidepressant behavioral responses. Biol. Psychiatry 74, 742-749.
96. Vollenweider, F.X., and Kometer, M. (2010). The neurobiology of psychedelic drugs: implications for the treatment of mood disorders. Nat. Rev. Neurosci. 11, 642-651.
97. Wacker, D., Wang, S., McCorvy, J.D., Betz, R.M., Venkatakrishnan, A.J., Levit, A., Lansu, K., Schools, Z.L., Che, T., Nichols, D.E., *et al*. (2017). Crystal Structure of an LSD-Bound Human Serotonin Receptor. Cell 168, 377-389.e12.
98. Whiteford, H.A., Degenhardt, L., Rehm, J., Baxter, A.J., Ferrari, A.J., Erskine, H.E., Charlson, F.J., Norman, R.E., Flaxman, A.D., Johns, N., *et al*. (2013). Global burden of disease attributable to mental and substance use disorders: findings from the Global Burden of Disease Study 2010. Lancet 382, 1575-1586.
99. Winter, J.C., Rice, K.C., Amorosi, D.J., and Rabin, R.A. (2007). Psilocybin-induced stimulus control in the rat. Pharmacol. Biochem. Behav. 87, 472-480.
100. Yang, C., Shirayama, Y., Zhang, J.C., Ren, Q., Yao, W., Ma, M., Dong, C., and Hashimoto, K. (2015). R-ketamine: a rapid-onset and sustained antidepressant without psychotomimetic side effects. Transl. Psychiatry 5, e632.
101. Yang, Y., Cui, Y., Sang, K., Dong, Y., Ni, Z., Ma, S., and Hu, H. (2018). Ketamine blocks bursting in the lateral habenula to rapidly relieve depression. Nature 554, 317-322.
102. Young, M.B., Andero, R., Ressler, K.J., and Howell, L.L. (2015). 3,4-Methylenedioxymethamphetamine facilitates fear

extinction learning. Transl. Psychiatry 5, e634.
103. Zanos, P., Moaddel, R., Morris, P.J., Georgiou, P., Fischell, J., Elmer, G.I., Alkondon, M., Yuan, P., Pribut, H.J., Singh, N.S., *et al*. (2016). NMDAR inhibition-independent antidepressant actions of ketamine metabolites. Nature 533, 481-486.
104. Zarate, C.A., Jr., Singh, J.B., Carlson, P.J., Brutsche, N.E., Ameli, R., Luckenbaugh, D.A., Charney, D.S., and Manji, H.K. (2006). A randomized trial of an N-methyl-D-aspartate antagonist in treatment-resistant major depression. Arch. Gen. Psychiatry 63, 856-864.
105. Zarate, C.A., Jr., Brutsche, N.E., Ibrahim, L., Franco-Chaves, J., Diaz-Granados, N., Cravchik, A., Selter, J., Marquardt, C.A., Liberty, V., and Luckenbaugh, D.A. (2012). Replication of ketamine's antidepressant efficacy in bipolar depression: a randomized controlled add-on trial. Biol. Psychiatry 71, 939-946.
106. Zeng, Y., Lv, F., Li, L., Yu, H., Dong, M., and Fu, Q. (2012). 7,8-dihydroxyflavone rescues spatial memory and synaptic plasticity in cognitively impaired aged rats. J. Neurochem. 122, 800-811.
107. Zubaran, C., Shoaib, M., Stolerman, I.P., Pablo, J., and Mash, D.C. (1999). Noribogaine generalization to the ibogaine stimulus: correlation with noribogaine concentration in rat brain. Neuropsychopharmacology 21, 119-126.

Supplemental Information

Supplemental Methods

Drugs

The NIH Drug Supply Program provided (±)-2,5-dimethoxy-4-iodoamphetamine (DOI), lysergic acid diethylamide (LSD), ibogaine (IBO), noribogaine (NOR), (±)-3,4-metheylendioxymethamphetamine (MDMA), psilocin (PSI), and D-amphetamine (AMPH). Other chemicals were purchased from commercial sources such as ketamine hydrochloride (KET, Fagron), serotonin hydrochloride (5-HT, Alfa Aesar), 7,8-dihydroxyflavone (DHF, TCI), ANA-12 (MedChem Express), rapamycin (RAPA, Alfa Aesar), ketanserin (KETSN, ApexBio), and brain-derived neurotrophic factor (BDNF, Sigma-Aldrich). The fumarate salt of *N*,*N*-dimethyltryptamine (DMT), was synthesized in house as described previously (Cameron *et al*., 2018) and judged to be analytically pure based on NMR and LC-MS data.

Neuritogenesis Experiments

After 3 days *in vitro* (DIV3), approximately 50,000 cells/well in poly-D-lysine coated 24 well plates were treated. Treatment was accomplished by first diluting DMSO stock solutions of compounds 1:10 in Neurobasal followed by a 1:100 dilution into each well (total dilution = 1:1000). After 72 h, cells were fixed by removing 80% of the media and replacing it with a volume of 4% aqueous paraformaldehyde (Alfa Aesar) equal to 50% of the working volume of the well. Then, the cells were allowed to sit for 20 min at room temperature before the fixative was aspirated and each well washed twice with DPBS. Cells were permeabilized using 0.2% Triton X-100 (ThermoFisher) in DPBS for 20 minutes at room temperature without shaking. Plates were blocked with antibody diluting buffer (ADB) containing 2% bovine serum albumin (BSA) in DPBS for 1 h at room temperature. Then, plates were incubated overnight at 4°C with gentle shaking in ADB and a chicken anti-MAP2 antibody (1:10,000; EnCor, CPCA-MAP2). The next day, plates were washed three times with DPBS and once with 2% ADB in DPBS. Plates were incubated for 1 h at room temperature in ADB containing an anti-chicken IgG secondary antibody conjugated to Alexa Fluor 488 (Life Technologies, 1:500) and washed five times with DPBS. After the final wash, 500 µL of DPBS was added per well and imaged on a Leica inverted epifluorescence microscope at 40x magnification. Images were analyzed using the Simple Neurite Tracer and Sholl analysis plug-ins for ImageJ Fiji (version 1.51N). Sholl analysis circle radii = 2 µm increments. All images were taken and analyzed by an experimenter blinded to treatment conditions.

For the dose response experiments (Figure S3) and two of the ketanserin blocking experiments (Figure 6G and H), a slightly modified method was employed. Neurons were cultured at approximately 15,000 cells/well in poly-D-lysine coated 96-well plates. For the dose response studies, neurons were treated at DIV3 by removing 10% of the media and replacing that with a 10x solution of compound in Neurobasal to reach the desired concentrations (final concentration of DMSO = 0.1%). For the ketanserin blocking experiments, the media was replaced on DIV3 with "replacement media" containing ketanserin. After 10 mins, compounds dissolved in Neurobasal were added to yield final concentrations of experimental compound and ketanserin (final concentration of DMSO = 0.2%). On DIV6, cells were fixed and imaged as described above. Plates were imaged on a Molecular Devices ImageXpress Micro XLS Widefield High-Content Analysis System at 9 sites per well using 20x magnification. Images were analyzed using ImageJ Fiji (version 1.51N). All analysis was done by an experimenter blinded to treatment conditions.

Spinogenesis Experiments

Cells were plated at a density of 35,000 cells/well on glass coverslips in 24 well plates. At DIV18, cells were treated for 24 h and fixed as described for the neuritogenesis experiments (vide supra). Fixative was aspirated and each well washed twice with DPBS. Cells were permeabilized using 0.2% Triton X-100 (ThermoFisher) in DPBS for 20 minutes at room temperature without shaking. Plates were blocked with antibody diluting buffer (ADB) containing 2% bovine serum albumin (BSA) in DPBS for 1 h at room temperature. Then, plates were incubated overnight at 4°C with gentle shaking in ADB and anti-chicken MAP2 (1:10,000; EnCor, CPCA-

MAP2). The next day, plates were washed three times with DPBS and once with 2% ADB in DPBS. Plates were incubated for 1 h at room temperature in ADB containing an anti-chicken IgG secondary antibody conjugated to Alexa Fluor 568 (Life Technologies, 1:500) and phalloidin conjugated to Alexa Fluor 488 (Life Technologies, 1:40). Then, the cells were washed five times with DPBS. Finally, the coverslips were mounted onto microscope slides using ProLong Gold (Life Technologies) and allowed to cure for 24 hours at room temperature. Images of secondary dendrites were taken using a Nikon N-SIM Structured Illumination Super-resolution Microscope with a 100x/NA 1.49 objective, 100 EX V-R diffraction grating, and an Andor iXon3 DU-897E EMCCD. Images were recollected and reconstructed in the "2D-SIM" mode (no out of focus light removal; reconstruction used three diffraction grating angles each with three translations). Dendritic spines were counted manually by a trained experimenter who was blinded to the treatment conditions.

Synaptogenesis Experiments

Cells were plated at a density of 35,000 cells/well on glass coverslips in 24 well plates. At DIV18, cells were treated for 24 h and fixed as described for the neuritogenesis experiments (vide supra). Fixative was aspirated and each well washed twice with DPBS. Cells were permeabilized using 0.2% Triton X-100 (ThermoFisher) in DPBS for 20 minutes at room temperature without shaking. Plates were blocked with antibody diluting buffer (ADB) containing 2% bovine serum albumin (BSA) in DPBS for 1 h at room temperature. Then, plates were incubated overnight at 4°C with gentle shaking in ADB and anti-MAP2 (1:10,000; EnCor, CPCA-MAP2), anti-VGLUT1 (Millipore, AB5905, 1:1000), and anti-PSD-95 (Millipore, MABN68, 1:500) antibodies. The next day, plates were washed three times with DPBS and once with 2% ADB in DPBS. Plates were incubated for 1 h at room temperature in ADB containing secondary antibodies conjugated to Alexa Fluor 488 (Life Technologies, 1:500), Cy3 (Jackson ImmunoResearch Inc, 1:500), or Alexa Fluor 647 (Jackson ImmunoResearch Inc, 1:500). Images of secondary dendrites were collected using a confocal microscope (Olympus FV1000) with a 60x oil objective and a 1.42 numerical aperture.

Synaptic density and size as well as PSD-95 and VGLUT1 densities were determined using custom software that works in three stages. The first stage is a foreground/background separation that outputs a mask of pixels within the image that correspond to the neuron. Next, puncta of synaptic proteins are identified using only pixels belonging to the foreground mask from the first stage. Finally, synapses are identified as colocalizations of puncta of pre- and post-synaptic proteins. The foreground mask is determined using a fluorescence intensity threshold chosen to maximize the connectedness of both the foreground and the background. Specifically, for a given threshold, connected pixels that pass the threshold are clustered together, and connected pixels that fall below threshold are clustered together. The average cluster size is computed for each type of cluster, and the threshold that maximizes the product of these averages is chosen. The resulting foreground mask is cleaned by removing clusters smaller than 0.06 μm^2 and smoothed by eliminating pixels connected to fewer than three other pixels that passed the threshold and adding pixels connected to more than four pixels that passed the threshold. Within the foreground mask, every pixel that has greater intensity than its neighbors is treated as a seed point for a potential punctum. The median and standard deviation of pixel intensities is computed for foreground pixels in the neighborhood of each seed point. The size of the local neighborhood is made dynamic in order to maintain sufficient statistics, with a minimum size of 5 μm^2. Seed points with intensities less than 3 standard deviations above the local median are rejected. For seed points that pass this threshold, adjacent pixels that pass a less stringent threshold (the minimum of 2 standard deviations above the median and the average of the median and seed point intensities) are clustered. In order to prevent neighboring puncta from being clustered together, intensities for newly added pixels are required to decrease if adjacent established pixels are already close to the lower threshold. Once the clustering is complete, puncta are smoothed in the same manner as the foreground and rejected if they are smaller than 0.03 μm^2. Pixels that are part of a punctum passing all of the above criteria are removed from the foreground mask so as not to be included in the threshold calculation for future puncta. After every seed point has been tested, those that failed are iterated over again until no new puncta are added. At the beginning of each iteration, puncta smaller the 3 times the minimum size threshold are removed to be reclustered. Synapses are defined as a colocalization of PSD-95 and VGLUT1 puncta. Two puncta are considered colocalized if they have at least 1 pixel of overlap. Synapse densities as well as the densities of presynaptic and postsynaptic markers are calculated using dendrite areas computed by counting pixels within a region of interest belonging to the foreground mask in the MAP2 channel. A similar approach for calculating synapse density has been described previously (Nielend *et al.*, 2014). Synapse size was calculated using the number of pixels representing each

colocalization event. Outliers were removed using the ROUT method in GraphPad Prism (version 7.0a) with a Q value equal to 5%.

ELISA

Cortical cultures were grown in 6-well plates (600,000 cells per well). At DIV17-18, all media was removed and replaced with fresh Neurobasal. After 4 h, each well was treated with compound dissolved in DMSO (1:1000) for 24 h. After the treatment period, the media was removed and the cells washed once with ice-cold DPBS. To each well was added 200 µL of Cell Extraction Buffer (Life Technologies) supplemented with cOmplete and PhoSTOP inhibitors, and incubated on ice for 5-10 min. Plates were scrapped and the contents collected. The samples were centrifuged at 10,000 x g for 10 min at 4°C and subjected to a BDNF ELISA assay (ThermoFisher) as per the manufacturer's protocol with the exception that the colorimetric signal was only allowed to develop for 8 minutes.

ddPCR

Cortical cultures were grown in 6-well plates (600,000 cells per well) until DIV17-18. At that time, cells were treated with compounds (1:1000 dilution from DMSO stock solutions) for 24h. Cells were then lysed using QIAzol Lysis Reagent (QIAGEN) and RNA extracted using the RNeasy isolation kit (QIAGEN) following instructions of the manufacturer. The resulting RNA was converted to cDNA using the iScript cDNA Synthesis Kit (BioRad). Droplets containing PCR master mix and taqman probes for BDNF (ThermoFisher, RN02531967_s1) and ESD (ThermoFisher, RN01468295_g1) were generated using the QX200 Droplet Digital PCR System (BioRad). Following PCR amplification, BDNF signal was quantified and normalized to the housekeeping gene ESD.

5-HT2A Staining Experiments

Cells were plated at a density of 35,000 cells/well on glass coverslips in 24 well plates. At DIV6 and DIV19, cells were fixed as described for the neuritogenesis experiments (vide supra). Fixative was aspirated and each well washed three times with DPBS. Cells were permeabilized and blocked using 0.1% Triton X-100 (ThermoFisher) and 5% goat serum (Vector Labs S-1000) in DPBS (TPG) for 1 hour at room temperature with gentle shaking. Plates were incubated overnight at 4°C with gentle shaking with anti-MAP2 (1:1000) and rabbit anti-5-HT_{2A} (Millipore Sigma PC176, 1:100) antibodies diluted in TPG. The next day, plates were washed three times for 5 min each with wash buffer (0.1% Triton X-100 in DPBS). Plates were incubated for 1 hour at room temperature in TPG containing secondary antibodies conjugated to Oregon Green 488 (Life Technologies, 1:500) and Alexa Fluor 568 (Life Technologies, 1:500). Plates were again washed three times for 5 min each with wash buffer (0.1% Triton X-100 in DPBS) and post-fixed for 10 min with 4% PFA in DPBS. Cells were washed three times with DPBS and mounted onto microscope slides using Prolong Gold (Life Technologies). After curing for 24 hours at room temperature, images of neurons were collected using a confocal microscope (Olympus FV1000) with a 60x oil objective (1.42 NA).

The anti-5-HT_{2A} antibody used in these studies (i.e., Millipore Sigma PC176) was produced using a peptide antigen corresponding to residues 22-41 of the rat 5-HT_{2A} receptor. The specificity of an antibody produced using the same antigen has been validated previously (Garlow *et al*., 1993). As it was unclear from the manufacturer's information whether or not the antibody utilized in our studies was produced using the same carrier protein (McDonald and Mascagni, 2007), we performed our own validation experiments. Briefly, HEK293T cells (ATCC, CRL-3216) and 198A2 cells (i.e., a HEK293 cell line stably expressing 5-HT_{2A} receptors, donated by Javier González-Maeso; see González-Maeso *et al*., 2003; Ebersole *et al*., 2003) were fixed, stained, and imaged with a 100x oil objective (1.3 NA) on an inverted widefield microscope (Leica DMIL). Representative bright-field images (grayscale) overlaid with fluorescence images (green) indicating 5- HT2A expression are shown below. The cells expressing 5-HT_{2A} receptors exhibit significantly more fluorescence and the expected staining at the cell membrane (white arrow), validating this antibody for immunofluorescence studies.

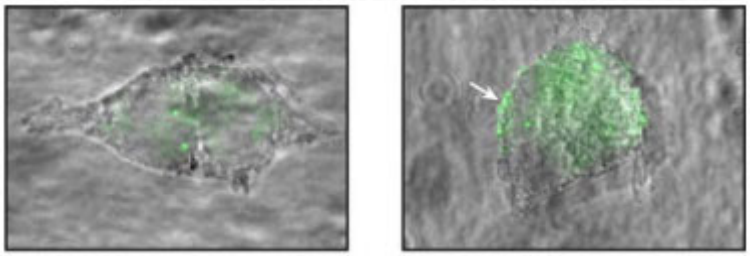

HEK293T
(Does Not Express 5-HT_{2A})

1988A
(Stably Expresses 5-HT_{2A})

Drosophila Experiments

For morphological analysis, we crossed *221-Gal4* with *UAS-cd4-tdGFP*, collected the progeny at either the first larval instar (early treatment) or late second larval instar (late treatment), then transferred the larvae to grape agar plates smeared with yeast paste. This yeast paste was dissolved in 1 mL of autoclaved water containing 0.1% DMSO with or without compounds dissolved at concentration of 10 µM. Whole, live wandering third instar larvae were mounted in 90% glycerol under coverslips sealed with grease and imaged using an Olympus FV1000 laser scanning confocal microscope. For fly stocks, we used the Gal4 driver line, *221-Gal4* (Grueber *et al*., 2003), to drive the expression of the membrane marker, *UAS-cd4-tdGFP* (Han *et al*., 2011), to visualize dendrite morphology for all conditions. Collected Z-stacks containing the dendritic arbors of the class I da sensory neurons were used for analysis. One neuron from segment A3 or A4 was imaged per larvae and three larvae were imaged per drug condition per treatment window (early vs. late treatment). All larval drug treatments were performed at least three separate times. Total dendrite length and the number of branch points were determined from maximum Z projections of the Z-stack image files using the Simple Neurite Tracer plugin for ImageJ Fiji (Longair *et al*., 2011). Data acquisition and analysis was performed by an experimenter blinded to treatment conditions.

Zebrafish Experiments

Wildtype fish (NHGRI-1) were dechorionated 24 h post fertilization (hpf) and placed individually into a 96-well plate containing chemicals of interest (10 µM compound, 0.1% DMSO). Larvae were raised in a light-cycled incubator (28°C) and subsequently subjected to an activity assay for 16 hours, from 5pm to 9am, at 5.5-6.5 days post fertilization (dpf). Specifically, they were imaged using DanioVision with a light cycle mimicking their natural day/night cycle. Subsequently, fish larvae (6.5 dpf) were immediately fixed following the movement assay using 4% aqueous paraformaldehyde overnight. Head-width measurements were performed by imaging larvae dorsally using a stereomicroscope (12x magnification) and a digital ruler (ImageJ) to measure the distance between the inner edges of each eye. Data acquisition and analysis was performed by an experimenter blinded to treatment conditions.

Golgi-Cox Staining

Female Sprague Dawley rats (~8 weeks old) were given an intraperitoneal injection of DMT, ketamine, or vehicle and sacrificed via decapitation 24 h later. Tissue was prepared following the protocol outlined in the FD Neurotechnologies Rapid GolgiStain Kit (FD Neurotechnologies) with slight modifications. Brains were stored in solution C for 2 months prior to slicing into 120 µm sections using a vibratome. These slices were placed onto microscope slides that were pre-coated with (3-aminopropyl)triethoxysilane. Slices were air dried for a week before staining. Slides were immersed in water twice for 2 minutes, DE solution for 10 minutes, and then water for 2 minutes. After this, slides were immersed sequentially in 25% ethanol for 1 minute, 50% ethanol for 4 minutes, 75% ethanol for 4 minutes, 95% ethanol for 4 minutes, and 100% ethanol for 4 minutes. Slides were then briefly dipped into xylenes before being mounted using DPX Mountant For Histology (Sigma), air-dried, and imaged on a Zeiss AxioScope. Spines were traced in three dimensions using Neurolucida software (version 10) at 100x magnification. Data acquisition and analysis was performed by an experimenter blinded to treatment conditions. Data represents individual neurons taken from 3 different animals per treatment,

Electrophysiology

Female Sprague Dawley rats (~8 weeks old) were given an intraperitoneal injection of DMT or vehicle. After 24 h, rats were anesthetized with isofluorane and transcardially perfused with ice-cold artificial cerebrospinal fluid (ACSF), containing 119 mM NaCl, 26.2 mM $NaHCO_3$, 11 mM glucose, 2.5 mM KCl, 1 mM NaH_2PO_4, 2.5 mM $CaCl_2$ and 1.3 mM $MgSO_4$. Brains were rapidly removed and 300 µm coronal slices from the mPFC were cut on a Leica VT1200 vibratome (Buffalo Grove, IL) with ice-cold ACSF solution. Slices were incubated in 32°C NMDG solution for 10 minutes, transferred to room temperature ACSF, and held for at least 50 minutes before recording. All solutions were vigorously perfused with 95% O_2 and 5% CO_2. Spontaneous excitatory postsynaptic currents (sEPSCs) were recorded at -70 mV in 32°C ACSF. Cells were patched with 3-5 MΩ borosilicate pipettes filled with intracellular solution containing 135 mM cesium methanesulfonate, 8 mM NaCl, 10 mM HEPES, 0.3 mM Na-GTP, 4 mM Mg-ATP, 0.3 mM EGTA, and 5 mM QX-314 (Sigma, St Louis, MO). Series resistance was monitored throughout experiments; cells were discarded if series resistance varied more than 25%. All recordings were obtained with a Multiclamp 700B amplifier (Molecular Devices, Sunnyvale, CA). Analysis was performed with the Mini Analysis program (Synaptosoft, Decatur, GA) with a 4 pA detection threshold. Data represents individual neurons taken from 3 different animals per treatment. Data acquisition and analysis was performed by experimenters blinded to treatment conditions.

Code Availability

The code used to generate synaptogenesis data is available from the corresponding author upon reasonable request.

Data Availability

The data that support the findings of this study are available from the corresponding author upon reasonable request.

Supplemental References

1. Ebersole, B.J., Visiers, I., Weinstein, H., and Sealfon, S. C. (2003). Molecular basis of partial agonism: orientation of indoleamine ligands in the binding pocket of the human serotonin 5-HT_{2A} receptor determines relative efficacy. Mol. Pharmacol. 63, 36-43.
2. Garlow, S.J., Morilak, D.A., Dean, R.R., Roth, B.L., and Ciaranello, R.D. (1993). Production and characterization of a specific 5-HT2 receptor antibody. Brain Res. 615, 113-120.
3. Grueber, W.B., Ye, B., Moore, A.W., Jan, L.Y., and Jan, Y.N. (2003). Dendrites of distinct classes of *Drosophila* sensory neurons show different capacities for homotypic repulsion. Curr. Biol. 13, 618-626.
4. Han, C., Jan, L.Y., and Jan, Y.N. (2011). Enhancer-driven membrane markers for analysis of nonautonomous mechanisms reveal neuron-glia interactions in *Drosophila*. Proc. Natl. Acad. Sci. USA 108, 9673-9768.
5. Longair, M.H., Baker, D.A., and Armstrong, J.D. (2011). Simple Neurite Tracer: open source software for reconstruction, visualization and analysis of neuronal processes. Bioinformatics 27, 2453-2454.
6. McDonald, A.J., and Mascagni, F. (2007). Neuronal localization of 5-HT type 2A receptor immunoreactivity in the rat basolateral amygdala. Neuroscience 146, 306-320.
7. Nieland, T.J., Logan, D.J., Saulnier, J., Lam, D., Johnson, C., Root, D.E., Carpenter, A.E., and Sabatini, B.L. (2014). High content image analysis identifies novel regulators of synaptogenesis in a high-throughput RNAi screen of primary neurons. PLoS One 9, e91744
8. González-Maeso, J., Yuen, T., Ebersole, B.J., Wurmbach, E., Lira, A., Zhou, M., Weisstaub, N., Hen, R., Gingrich, J.A., and Sealfon, S.C. (2003). Transcriptome fingerprints distinguish hallucinogenic and nonhallucinogenic 5-hydroxytryptamine 2A receptor agonist effects in mouse somatosensory cortex. J. Neurosci. 23, 8836-8843.